INVESTIGATION OF THE COMPOSITION OF SOLAR AND INTERSTELLAR MATTER USING SOLAR WIND AND PICKUP ION MEASUREMENTS WITH SWICS AND SWIMS ON THE ACE SPACECRAFT

G. GLOECKLER*, J. CAIN, F. M. IPAVICH and E. O. TUMS
Department of Physics, University of Maryland, College Park, U.S.A.

P. BEDINI, L. A. FISK and T. H. ZURBUCHEN
Department of Atmospheric, Oceanic, and Space Sciences, University of Michigan, Ann Arbor, U.S.A.

P. BOCHSLER, J. FISCHER and R. F. WIMMER-SCHWEINGRUBER
Physikalisches Institut, University of Bern, Switzerland

J. GEISS and R. KALLENBACH
International Space Science Institute, Bern, Switzerland

Abstract. The Solar Wind Ion Composition Spectrometer (SWICS) and the Solar Wind Ions Mass Spectrometer (SWIMS) on ACE are instruments optimized for measurements of the chemical and isotopic composition of solar and interstellar matter. SWICS determines uniquely the chemical and ionic-charge composition of the solar wind, the thermal and mean speeds of all major solar wind ions from H through Fe at all solar wind speeds above 300 km s^{-1} (protons) and 170 km s^{-1} (Fe^{+16}), and resolves H and He isotopes of both solar and interstellar sources. SWICS will measure the distribution functions of both the interstellar cloud and dust cloud pickup ions up to energies of 100 keV e^{-1}. SWIMS will measure the chemical, isotopic and charge state composition of the solar wind for every element between He and Ni. Each of the two instruments uses electrostatic analysis followed by a time-of-flight and, as required, an energy measurement. The observations made with SWICS and SWIMS will make valuable contributions to the ISTP objectives by providing information regarding the composition and energy distribution of matter entering the magnetosphere. In addition, SWICS and SWIMS results will have an impact on many areas of solar and heliospheric physics, in particular providing important and unique information on: (i) conditions and processes in the region of the corona where the solar wind is accelerated; (ii) the location of the source regions of the solar wind in the corona; (iii) coronal heating processes; (iv) the extent and causes of variations in the composition of the solar atmosphere; (v) plasma processes in the solar wind; (vi) the acceleration of particles in the solar wind; (vii) the physics of the pickup process of interstellar He in the solar wind; and (viii) the spatial distribution and characteristics of sources of neutral matter in the inner heliosphere.

*Also at: Department of Atmospheric, Oceanic, and Space Sciences, University of Michigan, Ann Arbor, U.S.A.

Space Science Reviews **86:** 497–539, 1998.

1. Introduction

The solar wind has now been observed for many decades and, while our knowledge of its properties and dynamics has increased tremendously over the years, a proper description of its origin and acceleration is still ahead of us. Measurements of the detailed composition of the solar wind are still relatively new but offer the best hope for solving this long standing problem, especially when combined with correlative remote sensing observations of the Sun's interior, surface, and atmosphere.

The discovery by SWICS on *Ulysses* of vast sources of both interstellar and interplanetary matter in the inner heliosphere, followed up by the initial discovery of He^+ by SULEICA on AMPTE, opened up a new avenue of galactic research and has produced knowledge far beyond expectations. At the 1 AU location of ACE, characteristics of the neutral interplanetary sources in particular can be studied to a degree not possible before and, in combination with observations with a nearly identical SWICS instrument on *Ulysses*, we have the unique opportunity to map the three-dimensional spatial distribution and the long term time variability of these sources.

The Solar Wind Ion Composition Spectrometer (SWICS) and the Solar Wind Ions Mass Spectrometer (SWIMS) on ACE will measure with unprecedented detail the chemical and isotopic composition of the solar wind as well as interstellar and interplanetary neutral matter under all conceivable solar wind flow conditions. We will derive routinely the bulk speeds, densities and kinetic temperatures* of the dominant solar wind ion species, and the charge state measurements will allow us to infer coronal temperatures. These experiments will also provide in-ecliptic, 1 AU baseline measurements of solar wind composition and conditions as well as the density of pickup helium (and probably oxygen and neon), important for interpretation of results from solar wind instruments on the *Ulysses* solar polar mission, as well as from space and ground based remote sensing observations of the Sun. SWICS and SWIMS will also characterize the matter entering the magnetosphere by measuring the elemental, isotopic, and charge state composition of the solar wind. The two instruments compliment each other, with SWICS providing elemental and charge state composition of the most abundant heavy solar wind ions under all circumstances. SWIMS, on the other hand, will determine with high mass resolution the elemental and isotopic composition of the solar wind over longer time scales and will measure the charge states of nearly every element between C and Fe in cold solar wind flows.

SWICS, the improved flight spare of SWICS on *Ulysses*, makes use of energy per charge analysis followed by the time-of-flight vs energy technique to determine both the mass per charge and mass of ions. Post-acceleration is used in order to measure the mass of ions of solar wind energies which otherwise would fall

*With the term 'kinetic temperature' we denote the second moment of the energy distribution function measured by the sensor. It should be roughly equivalent to the second order moment of the 3D-velocity distribution in the Sun–Earth direction.

below the threshold energy of the solid-state detectors. SWIMS, incorporating the best features of the MASS instrument of the WIND-SMS experiment and the MTOF instrument of the SOHO-CELIAS experiment, has high-mass resolution ($M/\Delta M > 100$) capabilities for measurements of the solar wind elemental and isotopic composition. SWIMS uses energy per charge analysis and acceleration or deceleration, followed by a time-of-flight measurement in a retarding, quadratically changing electric potential.

The design, fabrication, and testing of the SWIMS instrument was a collaborative effort involving the University of Maryland and the University of Bern. The SWICS experiment was modified at the University of Maryland using the *Ulysses* flight spare unit developed jointly by the University of Maryland, University of Bern, and the Max-Planck-Institut für Aeronomie. The combined DPU unit for SWICS, SWIMS, and SEPICA was developed by the Technical University of Braunschweig.

2. Major Scientific Objectives

Representative examples of major scientific problems the SWICS and SWIMS investigation on ACE will address are outlined below.

(1) Determine solar abundances by measuring with SWIMS the average elemental and isotopic composition of the solar wind in different solar wind flows found in the rise towards maximum portion of the solar cycle (e.g., in-ecliptic fast versus slow wind, CMEs, post-shock flows, etc.).

(2) Study solar wind acceleration, especially of heavy ions, using solar wind composition and charge state measurements made with SWICS with moderate time resolution.

(3) Study physical processes in the solar atmosphere, such as atom-ion separation in the upper chromosphere, by measuring with SWIMS the abundances of all elements below Ni, thus spanning the full range of first ionization potentials.

(4) Characterize the physical properties of the acceleration regions (in the lower corona) by measuring with SWICS and SWIMS the solar wind charge state distributions of several ion species (e.g., C, O, Mg, Si, and Fe).

(5) Study plasma processes affecting the solar wind kinetic properties and the velocity distributions of pickup and other suprathermal ions by measuring with SWICS the distribution functions of major ion species from $\sim$0.5 to $\sim$100 keV e^{-1}.

(6) Study interplanetary acceleration mechanisms producing shock-accelerated energetic storm particle events, CIR particles events, and upstream ions using measurements made with SWICS of the characteristics (composition and charge states) of the source particle populations.

(7) Provide stringent constraints on galactic chemical evolution over the past 4.6 Gy and deduce the primordial baryon density by determining with good preci-

sion the ^{3}He/^{4}He ratio both in the interstellar medium and in the fast and slow solar wind.

(8) Characterize the physical and chemical properties of the local interstellar cloud by determining with good precision the Neon and Oxygen abundance, the ^{22}Ne/^{20}Ne ratio, and the kinetic temperature of He and O atoms in this region.

(9) Determine the size, distribution, and strength of sources of neutral particles in the inner heliosphere by analyzing the velocity distribution functions of pickup C^+, O^+, and heavier singly charged ions for ion speed below the solar wind speed.

(10) In addition, SWICS and SWIMS measurements on ACE will provide the instantaneous characteristics of matter entering the Earth's magnetosphere through measurements of the mass, charge state, and energy distributions of solar wind and supra-thermal ions. The unique features of the ACE mission, including its complement of science instruments, make it possible to address a number of science topics and perform correlative studies with other ACE investigations. These include the study of dynamic processes in the foreshock region producing reflected, diffuse, and upstream ions, and acceleration of solar energetic particles.

The major scientific objectives of the SWICS/SWIMS investigation are discussed in some detail below.

2.1. STUDIES OF THE SOLAR CORONA

The acceleration of the solar wind and of solar energetic particles are topics of great interest but remain as yet to be fully understood. Solar wind acceleration models require a knowledge of boundary conditions (primarily temperature and density profiles) in the acceleration region and must make predictions that are consistent with all the measured properties of the solar wind at 1 AU. SWICS and SWIMS will provide information about some of the characteristics in the acceleration region, but of even greater importance will be the detailed characterization of the 1 AU solar wind in terms of composition and charge states, as well as bulk speeds and kinetic temperatures of some 40 ion types. Such measurements of the solar wind properties will play a crucial role in testing and constraining solar wind acceleration models, and should lead to a better understanding of where and how the solar wind is formed. Our current knowledge regarding solar wind composition measurements and models of solar wind origin is summarized by Fisk (1998) in this issue.

2.1.1. *Physical Processes in the Solar Corona*

The SWICS/SWIMS measurements will provide essential information on the conditions characterizing, and the physical processes operating in, that region of the corona where most of the solar wind and solar energetic particle acceleration occurs. The solar wind acceleration region is supposed to lie relatively high in the corona (typically $\sim$1–3 solar radii in altitude) where the density is very low, especially in coronal holes. Before SOHO, spectroscopic measurements of this region were difficult to obtain and many of the main questions are still an issue of much

debate (see, e.g., Habbal et al., 1995). As we discuss below, however, an abundance of information regarding the acceleration region is available from *in situ* measurements of solar wind and suprathermal ions. Indeed, it is quite convenient that the very particles whose acceleration and flow are being studied carry much of the necessary information within their composition and behavior.

When the ionization and recombination times characteristic of the dominant ion states of a particular ion species in the solar wind (e.g., the +6, +7, and +8 charge states of oxygen, the +4, +5, and +6 charge states of carbon, etc.) become long compared with the solar wind expansion time, the ionization state of that species becomes fixed (i.e., *frozen in*) and remains essentially unchanged as the ions flow through the heliosphere (Hundhausen et al., 1968). The relative abundances of the several ionization states of a particular ion species in the solar wind depend strongly on the electron temperature in the coronal region where the *freezing in* occurs. The measured ionization state of solar wind ions from SWICS and SWIMS will provide a direct measure of this electron temperature. The altitude at which the ionization state of solar wind ions is frozen-in is different for different ion species, as was inferred by SWICS *Ulysses* measurements (Geiss et al., 1995). For example, under typical coronal conditions, the ionization state of oxygen freezes in near 1.5 solar radii, whereas that of iron is not fixed until $\sim$3 solar radii. Because the ionization state depends so strongly on the electron temperature where freezing-in occurs, a comparison of the solar wind ionization states of oxygen with those of iron leads to a description of the radial profile of the coronal electron temperature. SWICS will measure not only the ionization state (or charge fraction) of O and Fe, but also of C, Mg, and Si, which will provide important information on the coronal temperature and the temperature gradient over a temperature range (from less than 10^6 K to much greater than 2×10^6 K). With SWIMS, charge states of elements such as Na, Al, Ca, and Cr will be observed.

2.1.2. *Acceleration of the Solar Wind*

The acceleration of heavy ions in the solar wind (helium and $Z > 2$) is expected to be different from the acceleration of the basic proton-electron plasma. Frictional coupling can be important in the heavy ion expansion (Bürgi and Geiss, 1986), and wave-particle interactions can have a different role in the acceleration of heavy ions than in that of protons (Hollweg, 1978). The composition, temperatures, and mean speeds of the solar wind minor ions measured by SWICS will reveal the effects of the several physical processes important in their expansion. These measurements will provide information concerning the overall proton-electron expansion, for they reveal the nature of the coronal environment in which both the heavy ions and protons are accelerated.

Frictional effects are likely to play an important role in the acceleration of heavy ions, as they serve to couple the heavy-ion expansion to the basic proton-electron expansion. The occurrence of frictional acceleration should be apparent in measurements of the mean bulk speeds of different ion species. If Coulomb interactions

are important, ions with large charge-squared-to-mass ratios should show evidence of preferential acceleration or deceleration. Other effects can preferentially alter particle speeds. For instance, a polarization electric field arising from electron-proton charge separation accelerates minor ions in proportion to their charge/mass ratio.

Wave-particle interactions and other processes in the corona may selectively increase the temperatures of heavy ions (relative to those of protons and electrons), thus facilitating their escape in the solar wind (e.g., Isenberg and Hollweg, 1983). Such heating processes may be reflected in the kinetic temperatures and mean flow speeds of heavy ions observed in the solar wind. Indeed, solar wind measurements have revealed that ions, at least in selected periods, tend toward equal thermal speeds, leading to an increasing temperature with increasing particle mass (Neugebauer, 1981; Schmidt et al., 1980; Ogilvie et al., 1980, Collier et al., 1996). With SWICS we will measure the kinetic temperatures and mean speeds of all major ion species including elements up to iron.

Heavy ions (as well as protons) may be directly accelerated through interaction with a wave field. In fact, this is almost certainly the case for the polar coronal hole wind (Geiss et al., 1995). The resonant acceleration of ions by Alfvén waves has been suggested as a potentially important process (Hollweg, 1978). Such processes may have various dependencies on the ion charge and mass, or no dependence whatsoever. Again, measurements of the mean flow speeds and temperatures of minor ions in the solar wind should reveal the occurrence of these processes.

2.1.3. *Atom-Ion Separation Processes*

It is well established that solar energetic particles (SEP) and solar wind elements that have first ionization potentials (FIP) less than $\sim$10 eV are over abundant relative to the corresponding photospheric abundances (e.g., Breneman and Stone, 1985; Gloeckler and Geiss, 1989). Therefore, a process seems to be operating that preferentially supplies the corona with elements that are easily ionized. An additional (and possibly related) mechanism appears to separate ions from neutrals on a time scale corresponding to their ionization rate and to preferentially feed the ionized fraction to the corona. Various models attempting to explain this so-called FIP effect have been proposed (e.g., von Steiger and Geiss, 1989; Geiss and Bürgi, 1986; Vauclair and Meyer, 1985), but none has been completely successful. The breakpoint that separates the *high* (normal abundance) and *low* (over abundant) FIP elements appears to be not a sharp step function, but rather a transition region that typically includes the elements carbon, sulfur, and phosphorus. Sometimes this region shifts in FIP to include elements such as oxygen. The magnitude of the relative abundance enhancement of the low FIP elements appears to vary, possibly as a function of solar wind type. For example, the solar wind from coronal holes appears to have only a small FIP effect, having a composition that most closely resembles that of the photosphere (Gloeckler et al., 1989; von Steiger et al., 1992). This could be a consequence of the different solar magnetic field conditions. With

SWICS and SWIMS we will study the temporal variation of the abundance of heavy ions in the solar wind, which will help in distinguishing among different modeling efforts. In particular, SWIMS will provide the continuous measurements of rarer elements and isotopes in the solar wind, including such elements as Ni, Ca, Al, and Na with low FIP (< 8 eV) and S and possibly P with a FIP in the transition region.

2.1.4. *Isotopic Composition of the Solar Wind*

Current measurements of solar wind isotopes heavier than helium are restricted, with a majority coming from lunar sample analysis and the foil collection technique (Geiss et al., 1972). SWICS will provide isotopic measurements for helium (^{3}He and ^{4}He) in the solar wind and the local interstellar cloud. With the SWIMS sensor we will obtain a continuous record of isotopic abundances of solar wind heavy ions (e.g., Ne, Mg, and Si). Solar wind isotopic abundance measurements with SWIMS will also allow for a direct correlation with simultaneous SEP isotopic measurements (by the energetic particle experiments ULEIS and SIS on ACE), which may resolve apparent disagreements in, e.g., the ^{20}Ne/^{22}Ne ratio (Geiss et al., 1972; Gloeckler and Geiss, 1989).

2.1.5. *Coronal Transients*

Coronal mass ejection (CME) events appear to originate (initially) in magnetically closed or quasi-closed coronal regions (e.g., Burlaga, 1984). The mass ejections from such regions move outward from the Sun to form a small but not insignificant part of the solar wind. (Fast CME-associated interplanetary shocks are the most dramatic solar wind manifestation of coronal transients in the low-latitude inner heliosphere.) As noted in the preceding sections, solar wind heavy ion measurements provide important information regarding the properties of the coronal region in which the wind originates. Hence, measurements by SWICS and SWIMS of heavy ions in solar wind plasma ejected as a coronal transient will give information regarding the properties of magnetically closed coronal regions, perhaps yielding important clues to the mechanism(s) whereby mass-ejection coronal transients are driven (e.g., Galvin et al., 1987). The interplanetary manifestations of these magnetically (quasi) closed structures sometimes include the bi-directional streaming of suprathermal ions (Marsden et al., 1987), which would be measured by SWICS.

2.2. STUDIES OF HELIOSPHERIC PHENOMENA

2.2.1. *Particle Acceleration*

Particles are accelerated in the solar wind up to energies $\sim$1 MeV nucl^{-1} by propagating shock waves that are generated by CMEs. They are also accelerated, particularly in solar-minimum conditions, in association with stream-stream interaction regions in the solar wind (Tan et al., 1989; Reames et al., 1991). During solar minimum conditions, the Sun produces relatively steady high-speed solar

wind streams, which, upon interacting with lower-speed wind at several AU from the Sun, accelerate particles that propagate back toward Earth in steady co-rotating particle streams. Each of these examples of acceleration is important to study since they can provide, by analogy, information on particle acceleration in large-scale astrophysical plasmas in less accessible regions of the universe.

Knowledge of the mass and the ionic charge, and thus of the rigidity, of the accelerated particles, and of their spectra over a wide energy range, can give answers to presently unsolved problems associated with the acceleration, viz., the source of the accelerated particles and the nature of the acceleration.

Particles accelerated in the solar wind could come directly from the solar wind plasma, or they could originate as more energetic particles of solar origin (such as high velocity tails of the solar wind), or as pickup ions. *Ulysses* observations (Gloeckler and Geiss, 1998) have shown that in the inner heliosphere, especially inside the orbit of Earth, the dominant sources of pickup ions are not interstellar atoms but could be neutrals desorbed from interplanetary dust as well as neutrals produced by evaporation of interstellar grains. If the former occurs, the requirements on the acceleration process are of course more severe. With the capability of SWICS to measure uniquely the composition of the solar wind and pickup ions, we can constrain the likely source of the accelerated particles.

As with solar flare and/or CME associated particles, the nature of acceleration processes in the solar wind is revealed in the rigidity and/or energy dependence of the spectra that they produce. SWICS, with its capability to measure the mass, the ionic charge, and the spectrum of ion species from H to Fe, will provide detailed constraints on these dependencies up to $\sim$100 keV charge^{-1}; i.e., the energy range from where the particles are injected into the acceleration process up to some of the higher energies obtained in typical events. Data from the SEPICA instrument, which can measure the charge states of more energetic particles, will allow us to examine these processes up to energies of several MeV nucl^{-1} to which ions are typically accelerated.

2.2.2. *Plasma Processes in the Solar Wind*

The SWICS and SWIMS experiments on ACE also provide the opportunity to investigate a variety of fundamental plasma processes in the solar wind. For example, there can be local heating of the solar wind at propagating shock waves or in stream-stream interaction regions; there can be instabilities driven by heat flux and other means. SWICS, with its capability of measuring the kinetic temperatures of all major solar wind ions, will provide an important probe of these processes. The dominant instabilities occurring can be revealed in the response of the kinetic temperatures of solar wind ions with different charge/mass ratios. As a simple example, when the ions cyclotron-damp the instabilities, the cyclotron frequency of the ions that absorb the most energy reveals the dominant frequency excited. Spectral measurements by SWICS and SWIMS will also reveal when and

how plasma processes generate extended suprathermal tails on the solar wind ion distributions.

2.3. DETAILED STUDIES OF PICKUP IONS

Heliospheric pickup ions are produced wherever there is a source of neutral molecules or atoms (see Gloeckler and Geiss, 1998; this issue). Ionized by solar UV and/or the solar wind, these newly formed ions are immediately accelerated by the $\mathbf{V}_{sw} \times \mathbf{B}$ electric field, gyrating about the ambient B field, thus forming a *ring*-type distribution in velocity space at $V = V_{sw}$ in the solar wind reference frame. Because pitch-angle scattering is weak (Gloeckler et al., 1995a; Fisk et al., 1997; Möbius et al., 1997), the spread into a *shell* distribution is far less rapid than previously assumed, leading to anisotropic distributions. Adiabatic deceleration in the expanding solar wind fills in the velocity space for $V < V_{sw}$ to a degree that depends on the spatial distribution of neutrals between the Sun and the observation point. Energy diffusion and acceleration to speeds beyond V_{sw} have been predicted (e.g., Isenberg, 1991), but is observed to be weak (Gloeckler et al., 1995a).

Pickup ions that have been observed so far include : (a) cometary pickup ions (e.g., Ipavich et al., 1986; Gloeckler et al., 1986), (b) interstellar pickup ions (Möbius et al., 1985; Gloeckler et al., 1993), (c) lunar pickup ions (Hilchenbach et al., 1991), and more recently (d) pickup ions from distributed inner sources of neutrals located inside several AU (Geiss et al., 1995). At the 1 AU orbit of ACE these inner sources will dominate, producing the largest fluxes of heavy pickup ions. Of the interstellar species only He, Ne and possibly O will be observable.

Thus, one of the principal objectives of SWICS on ACE will be the detailed mapping of the spatial distribution of these inner sources. This will be accomplished by measurements of the distribution functions of C^+, N^+, O^+, and perhaps some heavier ions over ion speeds from $\sim$0.6 to $\sim$2 times the solar wind speed. Because of adiabatic cooling, the speed of the pickup ions, V/V_{sw}, is uniquely related to the distance from the Sun, $R/R_\odot (R_\odot = 1$ AU) where they were picked up. Thus the density of neutrals at a distance $R (< 1$ AU) is determined from the pickup ion phase space density measured at the corresponding V/V_{sw}. In one orbit of ACE around the Sun we will obtain the spatial distribution of the neutral density of C, N, and O both in longitude and radial distance from the Sun. Subsequent orbits will allow us to examine solar cycle variability (if any) of these regions. Combining these ACE observations with similar measurements from SWICS on *Ulysses* at high latitudes will give us a truly three dimensional view of inner sources of pickup ions and will allow us to speculate on the origin of these sources.

The ACE orbit is optimum for detailed studies of interstellar pickup He. The neutral helium density is not reduced very much even at 1 AU from its interstellar value and gravitational focusing increases the flux of pickup He many fold in the *down wind* direction (Möbius et al., 1985, 1995). These statements also apply to Ne, although to a lesser degree. Among the prime objectives of the SWICS/

SWIMS investigation on ACE will be the more precise (than was possible with SWICS on *Ulysses*) measurements of the $^3He/^4He$ ratio in the local interstellar gas, a value of fundamental importance for models of Big Bang cosmology and galactic chemical evolution. In addition, the longitudinal distribution of interstellar neutral helium will be mapped using measurements of the fluxes of pickup He^+ and solar EUV flux provided by SOHO. This information, along with measurements of pickup He^+ made with SWICS on *Ulysses*, will allow us to infer the three-dimensional distribution of interstellar helium in the inner heliosphere, and to determine the ionization (loss) rate of neutral helium.

2.4. MULTI-MISSION STUDIES

2.4.1. *Long Baseline Measurements*

A SWICS sensor (Gloeckler et al., 1983, 1992) is successfully flying on the *Ulysses* spacecraft and is currently making detailed measurements of the elemental, ionic-charge composition and flow properties of solar wind and interstellar pickup ions at all heliographic latitudes (Gloeckler et al., 1993; Gloeckler, 1996). *Ulysses* was launched in October 1990 and began the out-of-the-ecliptic phase of the mission in February 1992. The first polar pass was completed in 1994. A comparison of solar wind elemental and ionic charge compositions at two different latitudes, and of the coronal conditions they imply, will be made using data from the two similar SWICS sensors on the two spacecraft.

We will use these simultaneous measurements from ACE (in the ecliptic) and *Ulysses* (out of the ecliptic) to help separate spatial and temporal variations and thus to determine how coronal conditions and processes vary with heliographic latitude and distance as discussed above.

2.4.2. *Short Baseline Measurements*

There are two instrument packages on currently active space missions which are very complementary to the SWICS and SWIMS sensors on ACE. On the satellite WIND, the SMS sensors measure the composition of the major components in the solar wind and some isotopes (for details, see Gloeckler et al., 1995b). Due to the fact that the distance between ACE and WIND is changing constantly due to differences in their respective orbits, the actual 3D structure of compositional boundaries can be mapped. For comparisons of isotopic and elemental abundances, data from the CELIAS sensors on SOHO will also be very interesting. Since SOHO is a three axis stabilized spacecraft, the geometrical factor of the instruments should be large (for details, see, Hovestadt et al., 1995). However, SOHO does not carry a magnetometer nor a 3D-plasma instrument and therefore the data analysis will be likely to rely on ACE data as well.

We will use these simultaneous measurements from ACE, WIND and SOHO to analyze spatial and temporal variations of the solar wind composition. We will therefore be able to determine the small-scale structure of coronal conditions rele-

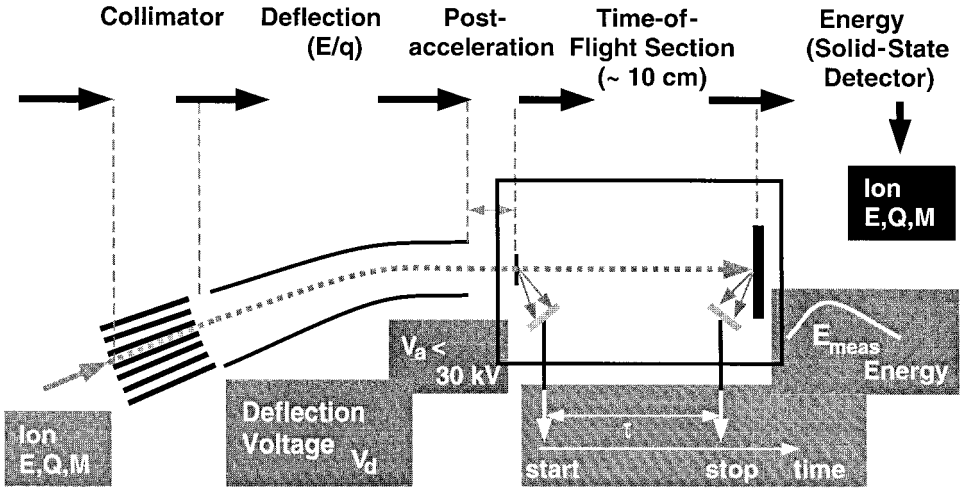

Figure 1. Schematic of the measurement technique used in SWICS, showing the functions of each of the five basic elements.

vant for the origin of the slow and fast solar wind and also of transient phenomena such as CMEs.

3. Instrument Descriptions

3.1. THE SOLAR WIND ION COMPOSITION SPECTROMETER (SWICS)

3.1.1. *SWICS Principle of Operation*

The operation of the SWICS sensor is based on techniques of particle identification using a combination of electrostatic deflection, post-acceleration, time-of-flight, and energy measurement (Gloeckler, 1977; Gloeckler and Hsieh, 1979; Gloeckler et al., 1992). Figure 1 shows schematically the principle of operation of SWICS and illustrates the function of the five basic sensor elements used:

(1) Ions of kinetic energy E, mass M, and charge (ionization) state Q enter the sensor through a large-area, multi-slit collimator that selects proper entrance trajectories of the particles.

(2) The electrostatic deflection analyzer serves both as a UV trap and an energy per charge (E/Q) filter, allowing only ions within a given energy per charge interval (determined by a stepped deflection voltage) to enter the time-of-flight vs energy system.

(3) Ions are post-accelerated by up to a 30 kV potential just before entering the time-of-flight vs energy system. The energy they gain is sufficient to be adequately measured by the solid-state detectors which typically have a 25 to 35 keV energy threshold. An energy measurement is required for determining the mass

composition of an ion population, and ions with energies below ∼30 keV must be accelerated if their mass is to be identified.

(4) In the time-of-flight (TOF) system the speed of each ion is determined by measuring the travel time τ of the particle between the start and stop detectors separated by a distance of 10 cm.

(5) The particle identification is completed by measuring the residual energy of the ions in a conventional low-noise solid-state detector.

From simultaneous measurements of the time-of-flight, τ, and residual energy, $E_{\rm meas}$, and a knowledge of E/Q and the post-acceleration voltage, U_a, we can determine the mass (M), charge state (Q), incident energy (E), or incident speed ($V_{\rm ion}$) of each ion as follows:

$$\begin{aligned} M &= 2(\tau/d)^2(E_{\rm meas}/\alpha), \\ Q &= \tfrac{E_{\rm meas}/\alpha}{(U_a+E/Q)\cdot\beta} \approx (E_{\rm meas}/\alpha)/U_a, \\ M/Q &= 2(\tau/d)^2(U_a + E/Q)\beta \approx 2(\tau/d)^2 U_a, \\ E_{\rm ion} &= Q\cdot(E/Q), \\ V_{\rm ion} &= 438\cdot[(E/Q)/(M/Q)]^{1/2}, \end{aligned} \tag{1}$$

where d is the flight path, β takes account of the small energy loss of ions in the thin foil of the start-time detector and α is the nuclear defect in solid state detectors (Ipavich et al., 1978). The units of $V_{\rm ion}$ are km s^{-1} when E/Q is in keV e^{-1} and M/Q is in amu e^{-1}. The approximate expressions for Q and M/Q hold for typical solar wind ions.

3.1.2. *Description of the SWICS Instrument*

The SWICS experiment consists of three separately mounted units which are electronically interconnected: the Sensor, the −30 kV Post Acceleration Power Supply (PAPS), and the Command and Data Translator (CDT). These units in turn contain various subsystems that will be described more fully below.

Sensor

A simplified cross-section of the SWICS sensor consisting of the deflection analyzer and the high-voltage bubble is shown in Figure 2.

The cylindrically shaped high-voltage bubble to which a post-acceleration voltage of up to −30 kV may be applied contains the TOF telescope and a proton/helium detector, the analog electronics, and the sensor power supplies. Each of these subsystems is supported by a G-11 insulator bulkhead and enclosed by a vapor-deposited, parylene-coated, machined-aluminum container. This container's outer surface is separated from the parylene-coated inner surface of the outer housing by a 6 mm gap.

The ultra-clean TOF compartment is physically isolated from the bubble electronics, with venting provided through the entrance slits and the collimator-deflection

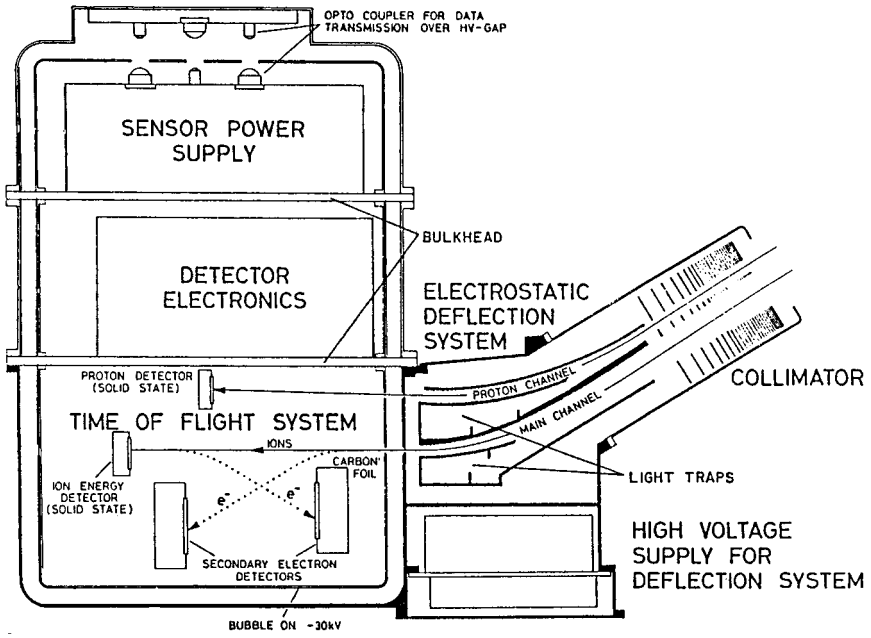

Figure 2. Cross-section of the SWICS sensor showing the collimator, the two-channel deflection system and its deflection power supply, the time-of-flight system and proton/helium detector, analog electronics, sensor bias and power supply, and opto-couplers for digital data transmission. The three inner compartments are supported by two bulkheads and are maintained at the post-acceleration voltage (-15 kV to -30 kV). The outer diameter of the cylindrically shaped outer housing is 15 cm.

system. Digital signals are transferred to the CDT across the 6 mm gap by six opto-couplers. The opto-coupler openings in the housings also serve as venting ports for the sensor electronics and power supplies. Power is supplied to the high-voltage bubble from the PAPS by means of an isolation transformer through a six-pin high-voltage feed-through (not shown) connected to the upper compartment. The photograph of the sensor (Figure 3) shows the outer configuration of the cylindrical bubble housing, the opto-coupler box, and the deflection system with the collimator opening covered by a dust/acoustic protective cover which swings open after launch. The gold-plated, cylindrically shaped container houses the -30 kV supply. The sensor is mounted on the top deck of the spacecraft, in the same orientation as shown in the photograph.

Deflection analyzer. The three-dimensional configuration of the deflection analyzer may be visualized by revolving the cross-sectional view shown in Figure 2 by 69° about the symmetry axis of the co-axial cylindrical sensor containers (HV bubble and outer shell). A single conical collimator (see Table 1 for details) services the two separate deflection regions of the analyzer. The multi-slit collimator is similar in construction to the collimator on our AMPTE instrument (Gloeckler et al., 1985) and allows us to extend the upper energy limit of our analyzer system to

TABLE I
Collimator and deflection analyzer characteristics for the SWICS sensor*

Sensor subsystem	Main channel	H/He channel
Collimator		
Type	conical	conical
Size		
Thickness (cm)	35	35
Slit area (cm^2)	87	31
No. of plates	18	18
Channel Configuration		
No. of channels	2960	1040
Cross-sectional area (cm^2)	3×10^{-3}	3×10^{-3}
Geometrical factor/channel(cm^2sr)	7×10^{-7}	7×10^{-7}
Sensor geometrical factor		
Isotropic (cm^2sr)	2×10^{-3}	7×10^{-4}
Directional (cm^2)	2×10^{-2}	9×10^{-3}
Deflection analyzer		
Type	small angle, conical with light trap	
Ion-optical properties		
Energy/charge range (keV/q)	0.49–100.0	0.11–15.05
Analyzer constant	12.46	15.93
Analyzer resolution	6.4 %	5.2 %
Analyzer dispersion	< 0.5 %	< 0.5 %
Deflection plates		
Configuration	serrated, black coated	
Shape	pie-shaped 70°	
Area (cm^2)	125	125
Gap (mm)	5 to 12	5 to 8
No. of voltage steps/cycle	60	60
Step size	1.0744/1.0365	1.0744/1.0365
Deflection voltage(V)	46.09–6300	6.91–945

*Note that the overall sensitivity of the integrated system depends not only on the geometrical factor of the subsystems, as given here, but is also dependent on the efficiencies of detecting various ions in the time-of-flight section.

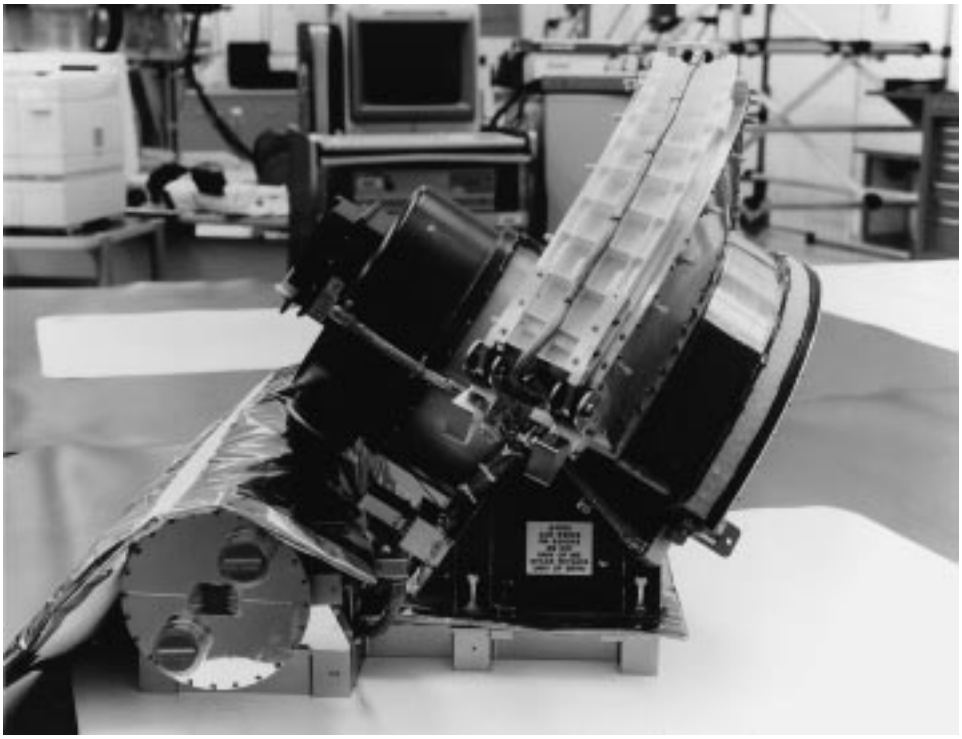

Figure 3. Photograph of the SWICS instrument.

$\sim$100 keV charge^{-1} while maintaining a reasonably large geometrical factor. The widths of the individual channels in the collimator are such as to limit dispersions in the analyzer and flight-path differences in the TOF system to $<$0.5%. The two inner deflection plates are connected to separate outputs of a variable voltage supply which is housed immediately below the deflection system and which typically increments the deflection voltage of both plates simultaneously in logarithmic steps. The maximum voltages on the upper and lower deflection plates are $+1$ kV and $+10$ kV, respectively. Serration, black-coating, and light traps are used to eliminate reflection of visible and UV radiation into the TOF system. Figure 4 shows a top view of the sensor with the electrostatic deflection plates and collimator plates exposed.

The smaller (upper) of the two deflection analyzer regions (proton/helium channel) normally covers an energy range from 0.16 to 15.05 keV charge^{-1}, has a resolution of 5.2%, and will routinely analyze solar wind protons, He, and heavier ions. These ions will be post-accelerated and will be counted by a single rectangular solid-state detector at two threshold levels 20–45 keV, and above 45 keV, corresponding to the energies of post-accelerated solar wind protons ($\sim$30 keV) and post-accelerated He and heavier ions ($>\sim$60 keV). As the voltage is stepped over the full range, this system provides separate E/Q spectra for solar wind

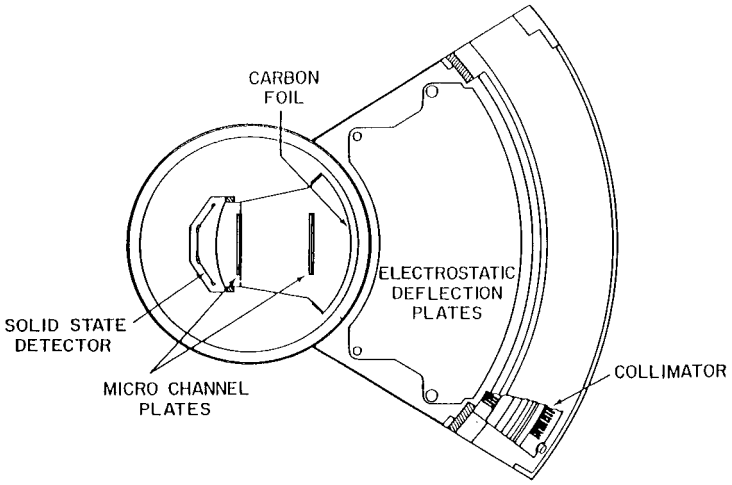

Figure 4. Top view of the SWICS instrument, showing the cross section of the time-of-flight telescope, and the positions of the three solid-state detectors, two microchannel plate assemblies, and the curved, grid supported carbon foil. The shapes of the deflection plates and the individual plates of the collimator are also shown.

protons and for solar wind He plus heavier elements, allowing us to determine in a simple manner, and at all solar wind temperatures, the bulk speed, density, and temperature of H^+ and He^{++} in the solar wind.

The larger (lower) deflection analyzer (main channel) has a 6.4% energy/charge resolution and is used for the full M vs M/Q analysis of solar wind He and heavier ions and of all suprathermal ions in the range 0.49–100.0 keV/charge. The TOF vs E system is placed behind the exit slit of the analyzer and inside the high-voltage bubble (Figure 2). At any given voltage step, the analyzer passes ions that have equal (to within the 6.4%) energy per charge. These ions are then post-accelerated and their mass, charge state, and energy measured by the TOF vs E system as described below.

Time-of-flight vs energy system. An important advantage of the TOF technique which measures the velocities of ions over a system which selects a narrow range of velocities (using, for example, crossed electric and magnetic fields) is that stepping over a velocity range is not required in our instruments. The TOF system accepts a wide range of velocities (or M/Q ratios) simultaneously, resulting in factors of 10 to 20 increases in both the time resolution and sensitivity. A second major advantage is that coincidence measurements used in TOF systems reduce background levels many orders of magnitude below the typical 10^{-2} to 1 count s^{-1} background measured in, for example, the singles rates of solid-state detectors on a typical spacecraft.

Figure 5 shows the cross section of the SWICS TOF vs E assembly consisting of a ‘start’ and ‘stop’ detector 10 cm apart. The start and stop signals are derived

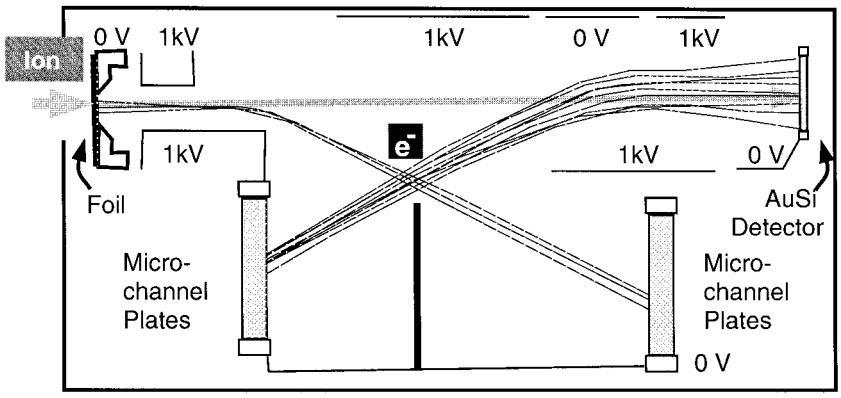

Figure 5. Cross section of the SWICS time-of-flight vs energy telescope showing computer-generated trajectories of secondary electrons emitted from the carbon foil and solid-state detector. The front surface of each of the two chevron-assembly microchannel plates (MCP) is biased slightly negatively with respect to the housing to repel low-energy (<100 eV) secondary electrons. A physical partition between the two MCPs prevents secondary electrons from one MCP triggering the other.

from secondary electrons (Gloeckler and Hsieh, 1979) which are released with a mean energy of a few eV when an ion enters or leaves a solid surface. The surface material used for the start detector is a thin foil (typically 1.5 μg cm^{-2} carbon foil supported on an 86% transmission nickel grid), and for the stop detector the gold front surface of the ion implant solid-state detector. The secondary electrons from the start and stop detectors are accelerated to $\sim$1 kV and then deflected by a system of acceleration gaps and deflection surfaces and strike the respective microchannel plate (MCP) assemblies, each of which consists of two rectangular MCPs in a chevron arrangement. A common supply (1 kV) is used to both accelerate and deflect the electrons. The output signals from the start and stop MCP assemblies are impedance matched and capacitively coupled across 4 kV in order to keep the foil and solid-state detector at local ground potential. The MCPs are normally biased at $\sim$3 kV to operate at a gain of about 2×10^6. This common bias voltage is adjustable by ground command. However, because both MCPs share the same bias supply, their gains cannot be separately adjusted.

The top view of the TOF vs energy telescope (Figure 4) shows the positions of the start and stop MCPs, the three solid-state detectors, and the curved carbon foil. The wide field-of-view and the three detectors are necessary to provide look-directions towards the Sun for all orientations of the ACE spacecraft. This also enables measurements of the suprathermal and pickup ion distribution functions over a large portion of phase space. The slight difference in the flight path of the secondary electrons introduces a timing uncertainty of $<\sim$0.2 ns FWHM, which is smaller than the $<\sim$ 0.5 ns FWHM resolution of the analog electronics. Ions are practically unaffected by the electric fields of the TOF assembly because of their

TABLE II
Time-of-flight and energy-system characteristics for the SWICS instrument

Subassembly	Characteristics
Time-of-flight assembly (TOF)	
Flight path of	10 cm
start element	carbon foil (1.5 μg cm^{-2}, grid supported)(0.4 $\times$ 8 cm^2)
Stop element of	3 rectangular solid-state detectors
main channel	(11.9 mm $\times$ 13.9 cm $\times$ 309 μm each)
Stop element of	1 rectangular solid-state detector
auxiliary channel	(6.0 mm $\times$ 6.6 mm $\times$ 309 μm)
Microchannel plates (MCP)	
Type	chevron stack
Size	2 rectangular (1.5 $\times$ 4.3 cm^2 each)
TOF telescope dispersion	
Path length, Δd/d	$<$ 0.005
Secondary electrons	0.3 ns
Energy measurement circuitry	
Range (keV)	35–600
Electronic noise (FWHM)	8 keV
E-ADC range	256 channels
E-ADC resolution	2.34 keV/channel
Time-of-flight measurement circuitry	
Range (ns)	10–180
Electronic noise (FWHM)	0.5 ns*
T-ADC range	1024 channels
T-ADC resolution	0.176 ns/channel

*Includes rms variations and drift of the analog electronics.

higher energy. The path-length dispersion $\Delta d/d$ for ions is negligible in the plane of Figure 5 and $<\sim$0.005 FWHM in the other direction.

The residual energy is measured by one of the three rectangular solid-state detectors. Table II gives additional details for the SWICS TOF vs E assembly.

Electronics

The SWICS electronics (see Figure 6) consists of an analog subsystem which is built into the central compartment of the high-voltage bubble (Figure 2), a variable deflection voltage supply and a detector/MCP bias supply both contained in the sensor, and the -30 kV post-acceleration power supply (PAPS) in its own cylindri-

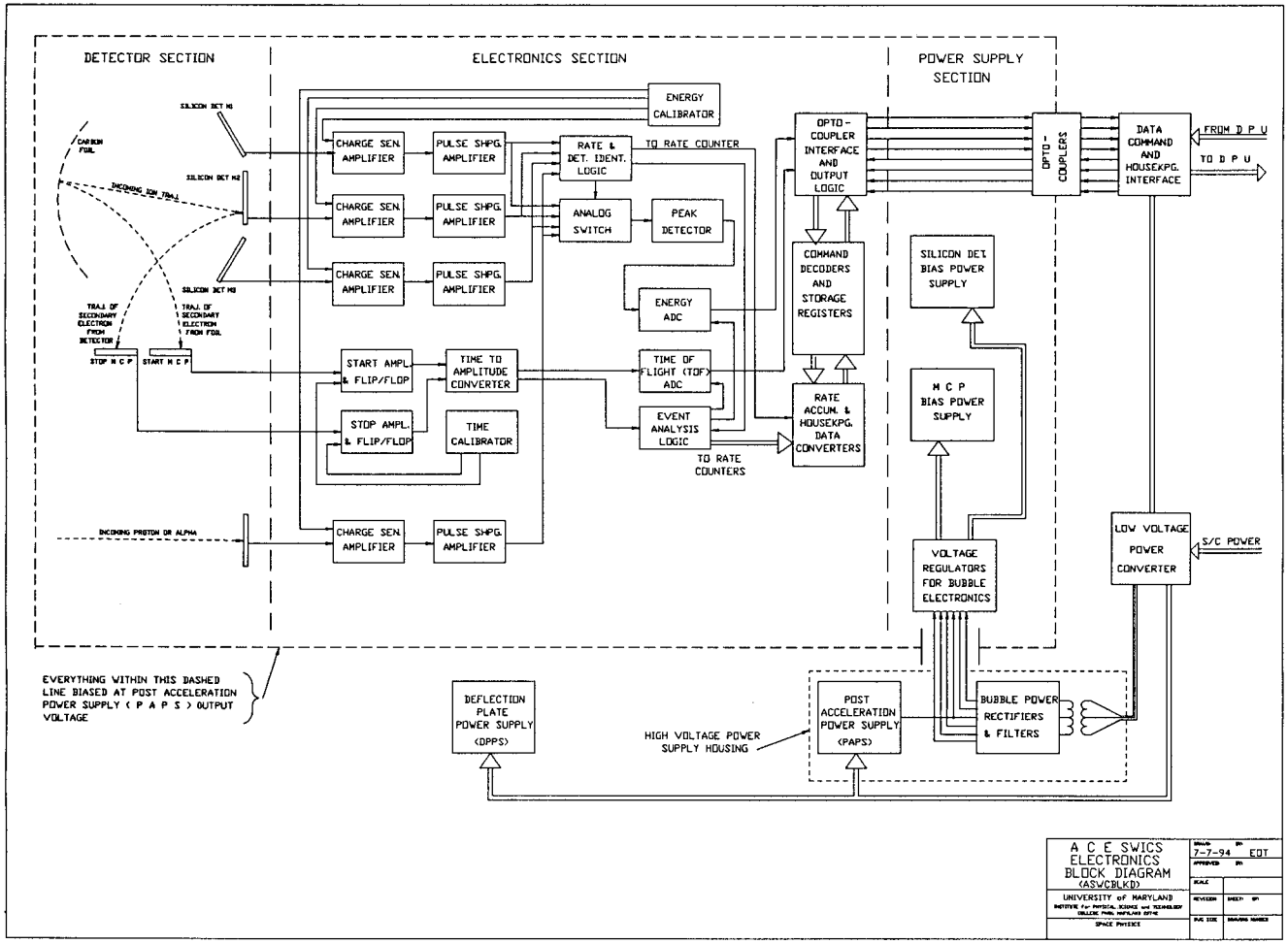

Figure 6. Electronics block diagram for the SWICS instrument.

cal housing. The Command and Data Translator (CDT) and the low-voltage power converter (LVPC) are mounted together in a housing beneath the sensor (not shown in Figure 2).

Analog electronics. The main function of the SWICS analog electronics is to measure the time-of-flight τ and energy E of ions triggering the TOF vs E system. In addition, solar wind protons and He are quickly identified and counted, and a number of coincidence conditions are established and their occurrence counted.

Time-of-flight measurement. Each MCP assembly output is capacitively coupled to a fast preamplifier whose function is to accept the 0.9 ns rise-time MCP output signals, shape, amplify, and feed them into a fast timing discriminator using tunnel diodes. The output signals from the start and stop timing discriminator are used as inputs to the Time-to-Amplitude Converter (TAC) which will produce: (a) an output pulse whose amplitude is proportional to the time interval between the trigger of the start and stop discriminators (T signal), and (b) a logic pulse (valid τ) provided the stop signal follows the start signal in $<$200 ns. The T signal is stretched and pulse-height-analyzed by a 10-bit 'Time' Amplitude-to-Digital Converter (T-ADC) with a 40 ns conversion time. The valid τ logic pulse is used to establish logic conditions and increment counting rates. We have measured the overall timing resolution of the analog electronics to be $<$0.2 ns when both the start and stop MCP pulses exceed 100 mV.

Energy measurement. The output of each of the three solid-state detectors of the TOF telescope is coupled to a low-noise (5 keV FWHM) preamplifier and shaping amplifier (unipolar pulses of 1 μs duration at 10%). All amplifiers have been hybridized to minimize weight and reduce cross talk. The output signals of each amplifier chain (E-signals) are pulse-height-analyzed by a common 8-bit 'Energy' Amplitude-to-Digital Converter (E-ADC) and are fed to respective threshold discriminators, whose output is used to identify the triggered detector and to establish logic conditions and increment counting rates. Two of the three main solid-state detectors (SSD) are ion implant SSDs, whereas the one farthest off the spin axis is a surface barrier SSD.

Solar wind proton/helium channel. The output of the low-noise H/He solid-state detector also goes through a preamplifier/shaping-amplifier chain which then feeds two threshold discriminators (20 keV and 45 keV) whose outputs increment the 'proton' and 'He' rate channels, respectively. It is possible to command the instrument into a mode such that the output of the H/He detector is analyzed instead of that of the three main telescope detectors. We also note that it is possible to select a deflection voltage stepping sequence that prevents solar wind protons from entering the time-of-flight system, but not the proton/helium channel.

TABLE III

SWICS telemetry allocation for data items generated in the analog electronics and S^3DPU

Data item	# per spin	Origin	Corresponding physical parameter	Bits per item per spin*	Bits per item per second
FSR	1×8	AE**	start detector rate	8×8	5.33
DCR	1×8	AE	start-stop coincidence rate (valid T)	8×8	5.33
TCR	1×8	AE	valid T - solid-state detector (SSD) coincidence rate	8×8	5.33
MSS	1×8	AE	combined count rate of three main channel SSDs	8×8	5.33
PROT	1×8	AE	solar wind proton rate	8×8	5.33
ALFA	1×8	AE	solar wind helium and heavy-ion rate	8×8	5.33
MEi	2	DPU	15 matrix elements, defined by up to 30 m vs m/q boxes	2×8	1.33
MRi	8×8	DPU***	counting rate of 8 selected ion species, defined by up to 20 m vs m/q boxes	64×8	42.67
BRi	4×8	DPU	4 sectored basic rates (incl. error rate), defined by up to 10 m vs m/q boxes	32×8	21.33
PHA	194	AE	194 24-bit E and T pulse-height events	194×24	388.00
HK	25	DPU	housekeeping data	25×8	16.67
Status	5	DPU	status bytes	5×8	40.00
Total					505.33 bit s^{-1}

*At the nominal spacecraft spin rate of 5.0 rpm the spin period is 12 s.
**AE = analog electronics.
***One set of the 15 sectored matrix elements (190 bytes) is collected over one complete voltage stepping cycle of 60 spins (12 min) and read out during the following cycle, 2 bytes per spin.

Monitor rates. The Monitor Rates are those rates produced in the analog electronics. The Front SEDA Rate (FSR) is incremented every time the Start detector is fired, the Double Coincidence Rate (DCR) indicates a valid τ, meaning that a Stop signal occurred within 200 ns of a Start signal, the Main Solid State (MSS) rate increments every time one of the three main solid-state detectors fires, and the Triple Coincidence Rate (TCR) counts when there is a valid τ signal in coincidence with an MSS count. The PROT and ALFA rates are, respectively, counts from 20–45 kV and greater than 45 kV discrimination of the proton/helium channel of SWICS.

Logic conditions and in-flight calibration. Table III lists the data items (rates and pulse heights) generated by the analog electronics. Pulse-height analysis of the

T signal is normally started by a valid τ signal whether or not an energy signal is present. Pulse-height analysis of the E signal normally requires a triple coincidence condition (start-stop and energy). It is possible, however, to change the T-ADC analysis logic by ground command to require also a triple coincidence for its analysis. An in-flight calibration provides on command a sequence of timing and amplitude pulses which are fed, respectively, to the fast amplifiers or preamplifiers of each MCP or solid-state detector. When the instrument is being calibrated, the trigger logic prevents all except the calibrator pulses from being analyzed.

3.2. THE SOLAR WIND ION MASS SPECTROMETER (SWIMS)

The Solar Wind Ion Mass Spectrometer (SWIMS) will determine the elemental and isotopic composition of solar wind ions over a wide range of solar wind conditions using a novel application of the time-of-flight measurement technique that results in exceptionally high mass resolution ($M/\Delta M > 100$). The high mass resolution SWIMS sensor will determine the abundance of nearly all of the chemical elements and most of their isotopes in the mass range 3 to 60 amu. SWIMS will measure the charge states of elements not resolved by SWICS, especially during periods of low kinetic temperature solar wind flow. The velocity range of the sensor is mass dependent, extending from ~200 to ~1000 km s^{-1} for C and from ~200 to ~500 km s^{-1} for Fe. This allows measurement of the abundances of the rarer solar wind species, including some elements heavier than iron and most isotopic ratios. The SWIMS sensor consists of an electrostatic deflection system, a time-of-flight High Mass Resolution Spectrometer (HMRS) (Hamilton et al., 1990; Gloeckler, 1990), associated high voltage supplies and low voltage power converter, and analog and digital electronics. A simplified cross section and block diagram of the SWIMS sensor is given in Figure 7. A photograph of the SWIMS instrument is shown in Figure 8.

3.2.1. *SWIMS Principle of Operation*

Solar wind ions of kinetic energy E, mass M, and ionization state Q enter the electrostatic deflection system which acts as an ultraviolet (UV) trap and an energy per charge (E/Q) passband filter. Ions which exit the deflection system have retained their original charge state and are confined to an energy per charge interval determined by the stepped deflection voltage.

Solar wind ions with an energy per charge E/Q corresponding to the value set by the deflection system enter the time-of-flight High Mass Resolution Spectrometer (HMRS) after passing through a thin carbon foil. In passing through the carbon foil, the ions reach charge equilibrium and emerge predominantly as either neutrals or singly charged ions, with a smaller fraction having charges $Q^* \geq 2$ or $Q^* = -1$.

The carbon foil (located at $z = 0$) also acts as the entrance to the TOF high mass resolution spectrometer. As the ion emerges from the foil, a small number (few to few tens) of secondary electrons are ejected from the foil. These electrons

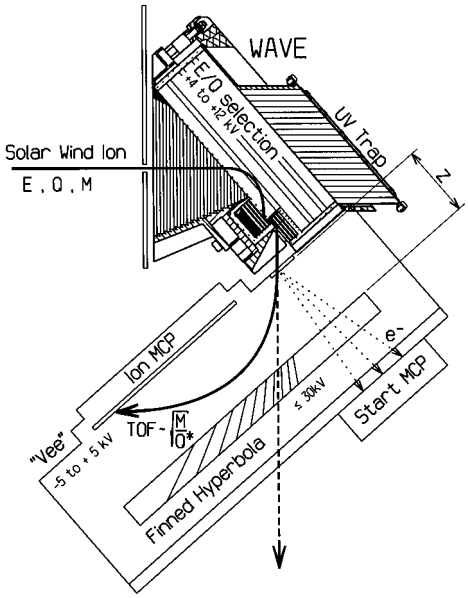

Figure 7. Cross-sectional schematic of the SWIMS instrument showing the WAVE entrance system, start MCP location, rail hyperbolic deflection surface, and position sensing stop MCP. A typical ion trajectory is shown.

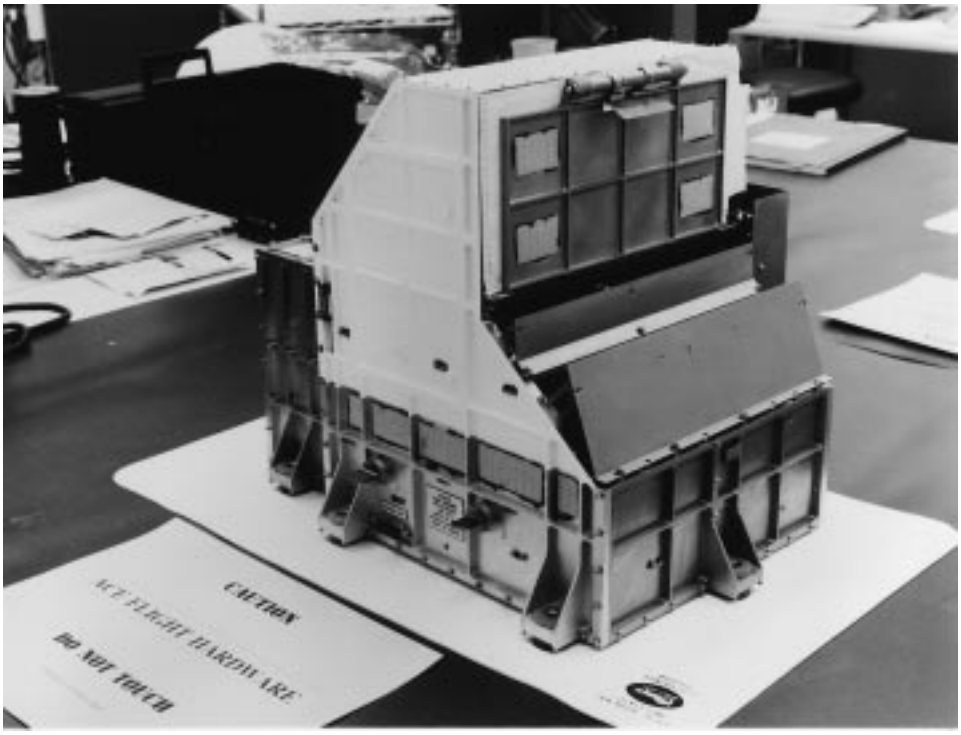

Figure 8. Photograph of the SWIMS instrument.

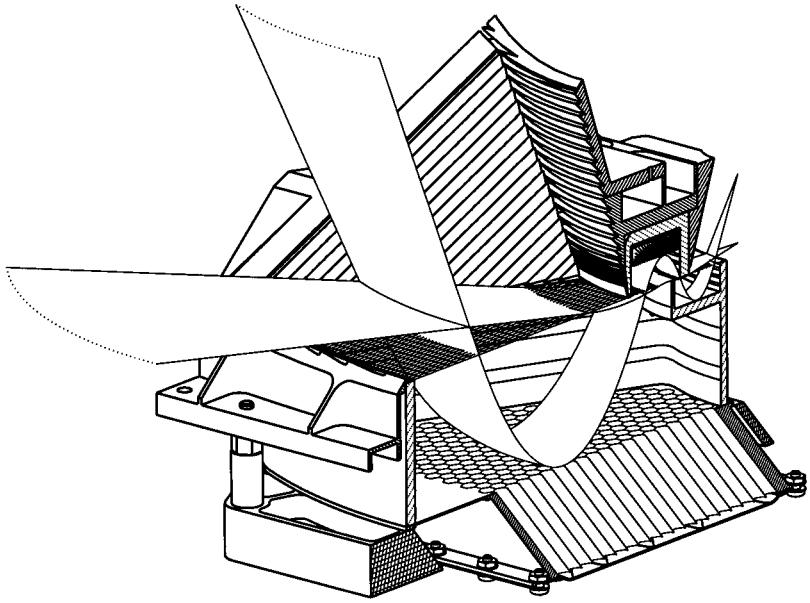

Figure 9. Cross section of the SWIMS deflection system. The two bands represent the effective field of view.

are accelerated to a microchannel plate assembly (MCP) and generate the start signal for the time-of-flight analysis. Positively charged ions are deflected back to a second, large area MCP assembly (also located at $z = 0$), thereby generating the stop signal for the time-of-flight analysis. The principle of operation of the mass analyzer is to measure the time-of-flight (τ) of the predominantly singly ionized particles in a static retarding harmonic electric potential ($V \propto z^2$, where z is the vertical distance from the carbon foil). In such a potential τ is independent of the magnitude and angle of the velocity of the emerging ion and depends only on its M/Q^* value:

$$\tau \propto (M/Q^*)^{1/2}, \tag{2}$$

Hence, a measurement of τ in this harmonic potential yields an unambiguous value of M/Q^* and, for $Q^* = 1$, of M. Typical times-of-flight range from 60 to 460 ns. Since τ can easily be measured with the precision of a fraction of a nanosecond, the ion mass is determined to a high degree of accuracy ($M/\Delta M > 100$). The required electric field is produced by a combination of a hyperbolic plate set at a large positive voltage V_H (typically 25 to 30 kV) and a V-shaped plate at ground potential (see Figure 10). The value of V_H determines the maximum ion energy that can be deflected by the electric field but does not affect the mass resolution.

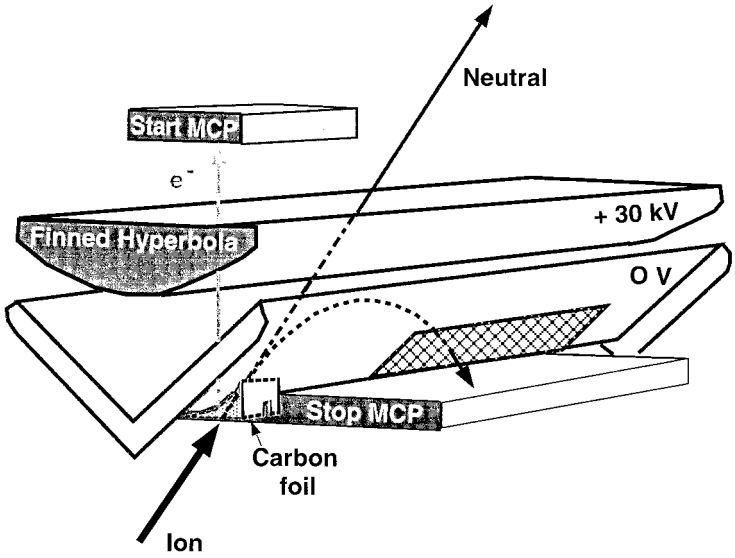

Figure 10. Schematic of the high mass resolution section of the SWIMS instrument. The high transparency of the hyperbola prevents neutrals from scattering onto the Stop MCP.

3.2.2. *Description of the SWIMS Instrument*

Unlike SWICS, the SWIMS instrument consists of one singly mounted box as shown in Figure 8. The assemblies contained in that unit are described below.

SWIMS deflection analyzer

Ions enter the SWIMS sensor through an entrance slit placed in front of the Wide-Angle, Variable Energy/charge (WAVE) passband deflection system. The WAVE deflection system is a wide angle electrostatic, multiple-chamber ion reflection system (see Figures 7 and 9) with the deflection plates connected to a stepped voltage supply. A black coated trap at the rear of the first (and largest) chamber prevents ultraviolet (UV) radiation from entering the time-of-flight analyzer. The entrance slit converts the WAVE system (which has a wide energy/charge passband of order one) to a narrow passband stepped deflection analyzer. The width and position of the entrance slit define the analyzer constant and energy passband ($\Delta(E/Q)/(E/Q) = 0.05$). The high voltage power supply steps the voltage on the reflection plates once per spin while the entrance grid is held at ground. The voltage steps are logarithmically spaced from 0.6 kV (0.5 keV e^{-1}) to 12.2 kV (9.5 keV e^{-1}) in 60 steps. The system has $\sim$5 % energy/charge resolution.

SWIMS Time-of-flight High Mass Resolution Spectrometer (HMRS)

Ions which exit the WAVE system have retained their original charge state and are confined to a 5% energy/charge band. Ions pass through a 4 mm$\times$15 mm grid-supported carbon foil (<2 μg cm^{-2}) cause emission of secondary electrons which are rapidly accelerated through a hole in the hyperbola (see Figure 10) and reach

the start chevron microchannel plate (MCP) assembly where their arrival time is recorded. Ions emerging from the start foil are most likely to have a 0 or +1 charge state with a much smaller fraction being +2 or (for some species) −1. Neutrals and negatively charged ions will strike the high voltage plate (hyperbola) of the HMRS. A finned hyperbola is used in order to suppress background caused by sputtering of those neutrals striking it.

A static harmonic potential region is created in the mass analyzer system between the finned, hyperbolically shaped positive potential plate and a V-shaped plate at relative ground potential. Positively charged ions emerging from the start foil will be deflected in this region and will hit the large area (100 mm × 15 mm) stop chevron MCP assembly. Because of the harmonic potential inside the mass analyzer, the times of flight of positively charged ions depend only on their mass/charge and, since most have charge state +1, only on their mass. The maximum voltage, V_H, of the hyperbolic deflection plate is +30 kV (but adjustable downward). The value of V_H determines the maximum ion energy that can be deflected by the electric field, but does not affect the mass resolution.

The anodes for both MCPs provide not only the required timing signals, but also amplitude signals that are pulse-height-analyzed by the electronics. These amplitude signals contain some information about particle mass and energy and will be used to further reduce residual background. In addition, the Stop MCP anode provides one-dimensional position information. This allows us to determine the approximate incident energy of an ion, from which its initial ionization state or charge Q may then be determined using the known E/Q setting of the deflection analyzer. The position information can also be used for additional rejection of background events.

SWIMS acceleration/deceleration system

The HMRS and its associated electronics are floated at an adjustable acceleration/deceleration potential V_F. This potential is adjusted once per spin and may be set negative to accelerate low-energy solar wind ions through the foil and thus increase the yield of +1 ions after the foil, or set positive to decelerate higher energy solar wind ions so that they are contained within the time-of-flight section. V_F has 256 linearly-spaced values from −5.0 to +5.0 kV. V_F is adjusted at each of the 60 steps of the WAVE deflection system to a preselected set of values related to the solar wind speed measured in the previous cycle.

SWIMS modes of operation

In its normal mode of operation the SWIMS deflection and acceleration/ deceleration voltages will be stepped once per spin. The deflection analyzer has 60 settings (0–59) with 5.1% separation between steps. The nominal sequence will comprise 60 steps starting with step 59 (9.5 keV e^{-1}) and ending with step 0 (0.5 keV e^{-1}). The acceleration/deceleration voltage will depend on the current step number and the speed of solar wind alpha particles measured during the previous cycle.

There will be optional modes in which any stepping sequence (of 60 steps) is selected. Such modes can be used to avoid (e.g., step over) the solar wind protons for most of the time and thus reduce fluence on the Start MCP. Another option is to set a given deflection voltage for each of the 60 steps in the sequence and specify the value of V_F. This option was used during calibration, for example.

Electronic and data system
The electronics for the SWIMS instrument (see Figure 11) consist of two digital and four analog boards that are packaged in an isolated box attached to the rear of the sensor. All circuitry dedicated to timing discrimination, internal calibrator operation, and pulse-height analysis of the Start and Stop microchannel plate signals are referenced to V_f, whereas the circuitry for the command/data interface to the S^3DPU are referenced to ground. The voltage difference between these two types of circuits is bridged by the use of opto-couplers.

Time-of-flight measurement. Fast preamplifiers accept the output signals from each of the two microchannel plate assemblies (Start and Stop), shape them, amplify them, and feed them to fast timing discriminators. The output from these discriminators are used as input to the Time-to-Amplitude Converter (TAC) which produces an output pulse whose amplitude is proportional to the time interval between the triggering of the Start and Stop discriminators, and a logic pulse if the Stop signal follows the Start signal within about 200 ns. The output pulse is shaped and pulse-height-analyzed by an Analog to Digital Converter (ADC), producing a 12-bit digital value. The logic pulse is used to increment counting rates.

Position and pulse-height information. Both Start and Stop micro-channel plate assemblies provide not only the required timing signals, but also amplitude signals that are pulse-height-analyzed by the electronics. These amplitude signals provide some information about particle mass and energy. In addition, the Stop MCP anodes provide one-dimensional position information, which allows us to determine the energy of an ion, and is also useful for rejecting background events. The position sensing is accomplished with a simple strip-strip anode composed of two interwoven electrodes of increasing and decreasing widths, respectively. The ratio of the signal from one electrode to the sum of the two signals indicates where along the anode an event occurs.

Power system
There are a total of eight power supplies in the SWIMS instrument, all located in the main sensor compartment. A Low-Voltage Power Converter (LVPC) accepts the spacecraft main bus 28V line and provides a variety of regulated and unregulated low voltages for the electronic circuitry. The Energy/Charge Power Supply (EQPS) outputs voltage up to 12 kV and is used to select ions of particular energy/charge. The V_f Power Supply (V_fPS) provides -5 kV to $+5$ kV for the acceleration or

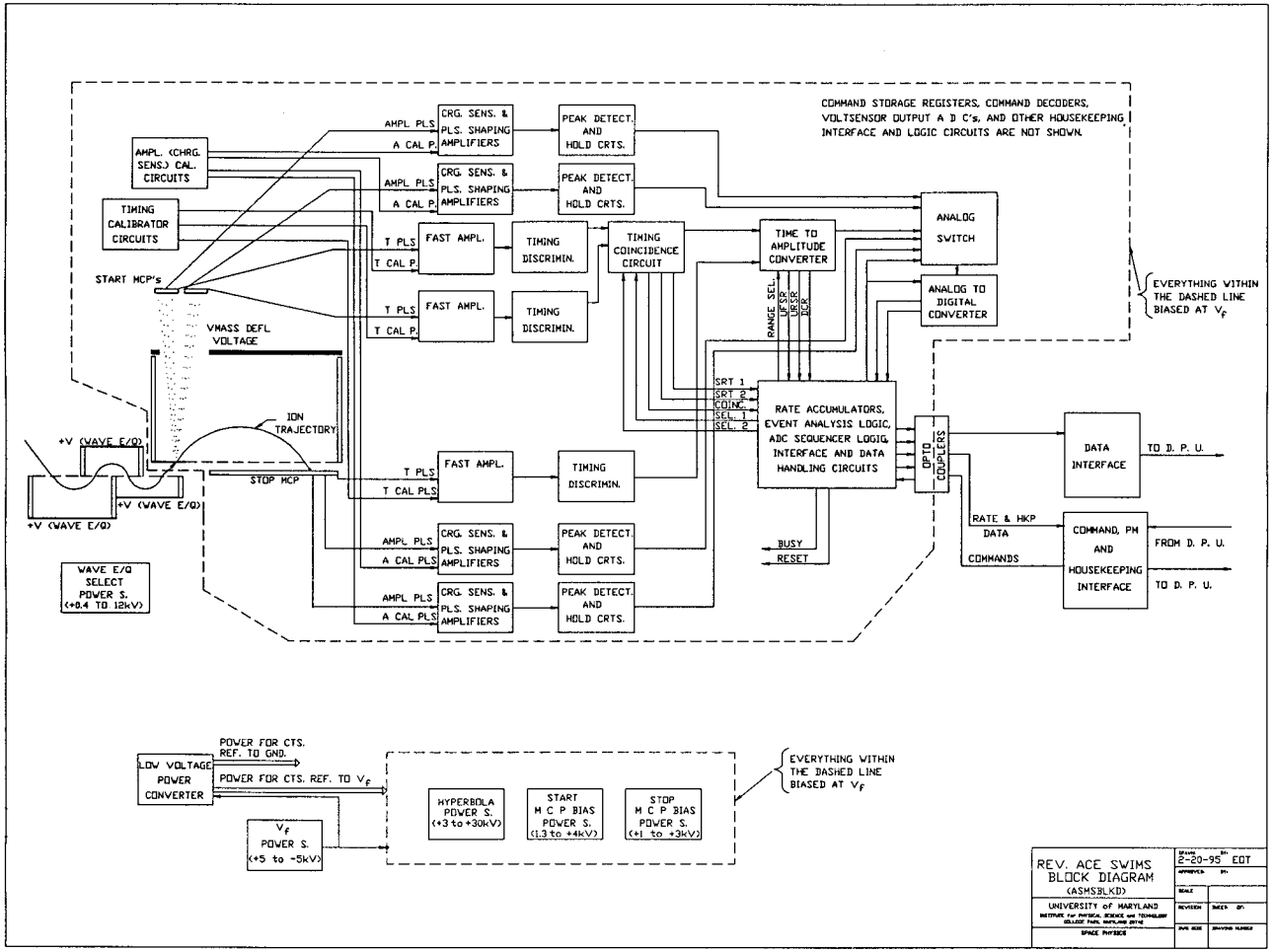

Figure 11. Electronics block diagram for the SWIMS instrument.

deceleration of these ions, respectively, and the Hyperbola Power Supply (HPS) provides up to 30 kV to the hyperbolic electrode in the HMRS to bend the ion trajectories down onto the Stop microchannel plate (MCP) assembly. For each of the two MCP assemblies there are two redundant power supplies so that at any one time either one set or another is operating. This is switchable by ground command. Unlike SWICS, the gain of each MCP assembly can be set independently by ground command to the power supplies.

3.3. FUNCTIONS OF THE DATA PROCESSING UNIT (S^3DPU)

Since a full description of the operation of the S^3DPU is given elsewhere (Möbius, et al., this issue), only aspects related to the SWICS/SWIMS operation will be discussed here. For each spin period of the spacecraft the S^3DPU produces an experiment data block containing housekeeping, rate, and pulse-height data for the SEPICA instrument, SWICS and SWIMS. For summary of the SWICS and SWIMS data items refer to Tables III and IV.

The basic pulse-height data (Time and Energy for SWICS; Time alone for SWIMS) provided by the sensors lend themselves to straightforward on-board processing which simplifies ground-based data reduction. The S^3DPU performs this function and provides the interface between the spacecraft and the SWICS and SWIMS instruments. The other principal SWICS- and SWIMS-related functions of the S^3DPU are to: (a) execute fast classification of ions according to the ion mass (M) and mass per charge (M/Q); (b) collect and store count-rate and pulse-height data, determine event priority, and execute appropriate event sequencing, compress the contents of each counting-rate register into an 8-bit floating-point representation, format all data into 8-bit words, and transfer this information to the spacecraft; and (c) perform all necessary control functions for the experiments, accept and execute ground commands, monitor the experiments status, and execute on-board calibration sequences of the analog electronics initiated by ground command.

3.3.1. *Fast On-board Classification of Ions and Rates*

For every ion for which pulse heights (T and E for SWICS; T for SWIMS) are available the S^3DPU executes fast classification according to ion mass and mass-per-charge (SWICS only) for collection and storage of ion species rates. Fast look-up table techniques are used to establish a correspondence between energy (E) and time-of-flight channel (T) pulse-height data contained in the SWICS event words and the positions of the mass (M) and mass-per-charge (M/Q) surfaces in the T vs E parameter space. For SWIMS only T and the hyperbola voltage are used. The classification algorithms used to generate the look-up tables is derived from the fundamental relations presented in Section 3.1 (SWICS) and Section 3.2 (SWIMS) and take into consideration several instrumental parameters such as the energy-per-charge value of the deflection voltage step, the post-acceleration voltage, the energy

TABLE IV

SWIMS telemetry allocation for data items generated in the analog electronics and S^3DPU

Data item	# per spin	Origin	Corresponding physical parameter	Bits per item per spin*	Bits per item per second
FSR	1×8	DPU**	start detector rate	8×8	5.33
FSRA	1×8	AE***	start detector rate – A anode (not used)	8×8	5.33
FSRB	1×8	AE	start detector rate – B anode	8×8	5.33
FSRAB	1×8	DPU**	start detector rate – A anode .AND. B anode (not used)	8×8	5.33
RSR	1×8	AE	stop detector rate	8×8	5.33
DCR	1×8	AE	valid start – stop coincidence	8×8	5.33
MFSR	1×8	AE	multiple FSRs rate	8×8	5.33
MDCR	1×8	AE	multiple DCRs rate	8×8	5.33
BRi	4×8	DPU	four basic rates, sectored	32×8	21.33
TOFi	35	DPU	two 1024-byte TOF rates are accumulated over one 60-spin cycle; 35 bytes are readout each spin of the following cycle	35×8	23.33
PHA	99	AE	99 48-bit pulse-height events	99×48	396.00
HK	35	DPU	housekeeping data	35×8	23.33
Status	5	DPU	status information	5×8	3.33
Total					510.0 bit s^{-1}

*At the nominal spacecraft spin rate of 5.0 rpm the spin period is 12 s.
**The S^3DPU determines if FSR=FSRA, FSRB, or FSRAB. This is changeable by ground command.
***AE = analog electronics.

loss in the carbon foil, and (for SWICS) the pulse-height defect in the solid-state detector. The M and M/Q values for SWICS returned by the classifier are used to increment appropriate storage registers corresponding to Basic Rates, Matrix Rates, and Matrix Elements. For SWIMS only Basic Rates are collected.

Directional information

The S^3DPU uses the spacecraft spin clock and Sun pulse to apportion the azimuthal (spacecraft) plane into eight equally sized sectors, nominally 45° each. For each type of rate (Monitor, Basic, Matrix, and Element) the S^3DPU collects eight rates per spin period – one for each of the azimuthal sectors.

Basic rates

For SWICS, Basic Rates correspond to counting rates of ion species groups that fall into specified regions of E - τ (or τ only) space defined by coarse resolution rectangular 'boxes' in M vs M/Q or upper and lower limits in M/Q space when

no E is measured. For SWIMS these rates are defined by upper and lower limits in each of the four pulse-height data items: Time-of-flight τ, Start Amplitude A, Stop Amplitude K, and Stop Position X. The boundaries of all boxes are defined in S^{3}DPU internal tables that can be uploaded by ground command. A Basic Rate is incremented by the S^{3}DPU when the M and M/Q calculated for an event word fall within the appropriate pulse-height range. These rates are used for the normalization of the direct pulse-height words (see section below on direct pulse-height analysis). For SWICS a maximum of four Basic Rates can be defined, using a maximum of 10 box definitions. For SWIMS there are also four Basic Rates.

Matrix rates (SWICS only)
Matrix rates correspond to the counting rates of selected ion species defined by medium resolution rectangular 'boxes' in M vs M/Q space or upper and lower limits in M/Q space when no E is measured (so called 'mass zero' events). The boundaries of these boxes are defined in a S^{3}DPU internal table which can be uploaded by ground command. A Matrix Rate is incremented by the S^{3}DPU when the M and M/Q (or only M/Q) calculated for an event word fall within the appropriate pulse-height range. A maximum of 8 Matrix Rates can be defined, using a maximum of 20 box definitions. Positions of the Matrix Rates in M vs M/Q space are shown in Figure 12 overlaid on raw flight data discussed below.

Matrix elements (SWICS) and time-of-flight spectra (SWIMS)
For SWICS, Matrix Elements (and for SWIMS, T Spectra) are fine resolution Matrix Rates that are collected over an entire deflection voltage stepping cycle (60 spins) and read out during the following cycle. As a result, information indicating the voltage step (hence E/Q) over which a particular event occurred is not retained. The boundaries of these boxes (upper and lower limits in M and M/Q) are defined in a S^{3}DPU internal table which can be uploaded by ground command. For SWICS a maximum of 15 Matrix Elements can be defined, using a maximum of 30 box definitions. For SWIMS there are two 1024-byte Time-of-flight Spectra that are defined by upper and lower limits in Start Amplitude A, Stop Amplitude K, and Stop Position X. The Stop Amplitude K is the sum of the amplitudes for the two electrodes ($k1$ and $k2$) of the Stop position-sensing anode. The Stop Position X is defined as $k1/(k1 + k2)$.

3.3.2. *Direct Pulse-Height Analysis Data and Priority Selection*
The most detailed information about the composition, arrival direction, and energy of ions is contained in the pulse-height analysis (PHA) words. For SWICS each word is 24 bits long: 8 bits for energy, 10 bits for time, 3 bits to indicate in which of eight sectors the event occurred, and 3 bits to identify both the priority and the associated detector. The SWIMS PHA word is 48 bits long: 12 bits time, 10 bits each for Start Amplitude, Stop Amplitude, and Stop Position, and 3 bits each for Range (priority category) and Sector information. Nominally the S^{3}DPU records

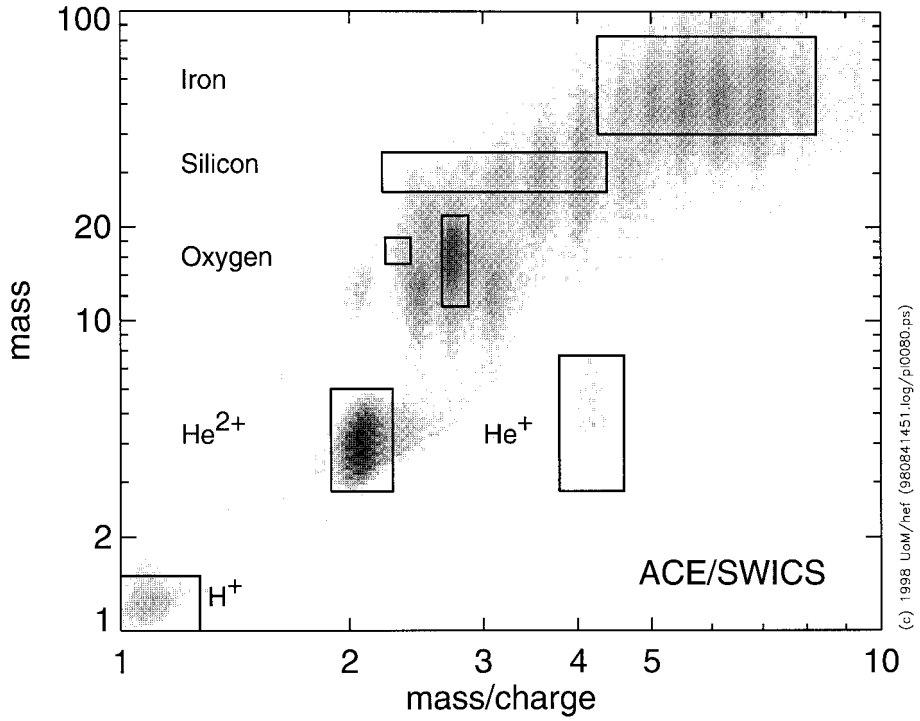

Figure 12. Matrix rate box definitions overlaid on flight data. These definitions are used by the S^3DPU to calculate rates which are also used for the calculation of browse parameters.

194 SWICS pulse-height events each spin period, and 99 SWIMS events. The priority categories are defined by the Basic Rates (see discussion of Basic Rates above).

4. Instrument Requirements

4.1. TELEMETRY AND COMMAND

On-board processing reduces considerably the telemetry that would otherwise be required to send back the information acquired by the sensors. The telemetry required to transmit the basic rates, matrix rates, matrix elements, and direct pulse heights is given in Tables III and IV. The total bit rate for SWICS is 505 bit s^{-1}, and for SWIMS is 510 bit s^{-1}. The instruments are controlled by a total of four spacecraft relay commands each: instrument power, operational heater power, survival heater power, and pyro power (for opening of the acoustic cover). Sensor configuration and deflection voltage sequencing is accomplished by the S^3DPU, which sends the current set of sensor commands to the sensors every 1.5 s. (That set of commands is changed by ground command to the S^3DPU.)

4.2. CLEANLINESS AND THERMAL

Because of the susceptibility of the MCPs and solid-state detectors to contaminants and because thin foils are employed in both sensors, dust/acoustic covers are utilized. These covers were commanded to swing open after the spacecraft was injected into its orbit. To avoid damage to the MCPs prior to launch, the instruments were purged continuously with dry nitrogen through ports provided in the sensors.

Thermal-design requirements for SWICS and SWIMS are an orbital temperature of -25° C to 0° C, preferably -20° C to -10° C. For SWICS the thermal requirements are driven by solid-state-detector operating and survival temperature limits. For SWIMS the requirements are governed by the operating limits of the telescope assembly since high temperatures lead to a high background due to the ionization of outgassed water. The requirements are achieved through use of thermal reflecting coatings, blankets and radiators, and operational heaters.

5. Instrument Capabilities and Performance

The SWICS and SWIMS instruments are capable of measuring the solar wind elemental, isotopic and charge-state composition under all conceivable solar wind conditions. The sensitivity and dynamic range of the instrument are such that the mean speeds, temperatures, and densities of the major elements in the solar wind may be determined with a time resolution of 12 min to $\sim$1 hr.

5.1. ENERGY RANGE

For SWICS the combined energy range of the main channel and the H/He channel extends from 110 eV/q (145 km s^{-1} for protons) to 100 keV/q (4380 km s^{-1} for protons; 1660 km s^{-1} for Fe^{8+}). This large dynamic range of 1000 in energy per charge will allow us to carry out solar wind composition measurements under all possible flow conditions, as well as to study pickup ions and the suprathermal tails of the distribution functions of, for example H, He, and O. Combining SWICS and SWIMS data allows the determination of charge state distributions of isotopes that can not be resolved by SWICS alone.

5.2. SENSITIVITY

The multi-slit collimator used in SWICS makes it possible to obtain a large geometrical factor and a wide field-of-view without sacrificing the energy resolution of the deflection analyzer. Since SWICS will predominantly measure solar wind ions, the relevant measure of sensitivity is related to the effective area presented to an incoming parallel beam (see Table I). The entrance system of SWIMS allows particles to enter from a wide range of angles.

The counting efficiencies in both TOF systems depend on the degree of scattering of ions in the front foil (most pronounced for low-energy heavy ions) and the number of secondary electrons produced by ions at the surface of the foil. The SWICS efficiency also depends on the secondary electron production by the solid-state detector (lowest number for higher energy protons). For SWIMS the efficiency depends on the charge state of the ions after passing through the carbon foil. The majority of the incident ions become neutrals as they pass through the carbon foil. In order to minimize the background caused by reflected neutrals, a finned hyperbola was used to allow the neutrals to be trapped. As a result SWIMS operates with a very low background.

We have calibrated SWICS and SWIMS using beams of selected ions available prior to launch from H through Kr. Some of our results of efficiencies are presented in Section 5.5 below.

5.3. INTENSITY DYNAMIC RANGE

With the SWICS and SWIMS instruments we are able to achieve an intensity dynamic range of $\sim 10^9$ because: (a) the most intense solar wind fluxes (protons) are generally measured only in the SWICS H/He channel; (b) the rare elements are analyzed in the TOF systems with high priority; and (c) the high immunity to background makes it possible to detect and identify rare elements and isotopes. The maximum proton flux of $\sim 10^9$ cm^{-2} s^{-1} that we can measure is determined by the peak counting rate of our H/He detector ($\sim 5 \times 10^5$ count s^{-1}), the proton temperature, and the energy bandwidth and geometrical factor of the deflection analyzer.

5.4. MASS AND MASS-PER-CHARGE RESOLUTION

We have determined the mass and mass/charge resolution of SWICS for every major ion species using all known aspects of the instrument. These include effects due to: (a) deflection-analyzer system resolution and dispersion; (b) electronic noise in the TOF measurement and path-length dispersion of secondary electrons; (c) path-length differences of ions in the TOF system; (d) energy dispersion associated with nuclear defects in solid-state detectors and electronic noise in the energy measurement; and (e) timing dispersions caused by energy straggling of ions in the carbon foil. These effects which have been measured or are determined by the geometry of the system are combined in quadrature to give the FWHM resolutions in mass, (M), and mass/charge, (M/Q). Table VI summarizes the mass and mass/charge resolution in SWICS for common solar wind ions.

For SWIMS the mass resolution Δ_M is roughly proportional to $\sqrt{M}$ and also depends somewhat on the scattering of ions in the carbon foil. In general, $\Delta_M/M <$ 0.02).

TABLE V
Mass and power for SWICS and SWIMS

Subsystem	Mass (g)	Power (mW)
SWICS		
−30 kV supply (PAPS)	**566**	**550**
Sensor	**3426**	**1900**
Deflection system and deflection supply	1483	400
Analog electronics and bias supply	908	1200
Sensor elements and structure	1035	300
CDT Assembly	**1698**	**2500**
CDT	800	1000
Low-voltage power converter	800	1500
Thermal blankets	**280**	
SWICS total	**5970 g**	**4950*** **mW**
* Average power; peak power 6.11 W		
SWIMS		
WAVE entrance system	**586**	
Sensor	**7014**	**6800**
Power supplies	1450	2850
Analog/Digital electronics	980	3950
HMRS telescope	740	
Structure, etc.	4044	
Thermal items	**450**	
SWIMS total	**8050 g**	**6800**** **mW**

**Average power; peak power 7.2 W

Examples of the mass (SWICS and SWIMS) and mass/charge (SWICS only) resolution are shown in Figure 13 for SWICS and Figure 14 for SWIMS which show raw flight data.

5.5. INSTRUMENT CALIBRATION

The SWICS instrument on ACE is the improved flight spare unit of SWICS on *Ulysses* (Gloeckler et al., 1992), launched in 1990, and is similar to SWICS on WIND (Gloeckler et al., 1995b) launched in 1994. SWIMS is an improved version of the SOHO CELIAS-MTOF instrument, (Hovestadt et al., 1995) launched in 1995, incorporating energy per charge analysis used in the MASS instrument on WIND. There is preflight calibration and flight data available for these instruments allowing for cross checking of instrument responses. Pre-flight calibration

TABLE VI
SWICS resolution characteristics for typical solar wind ions*

Element	Mass (amu)	Charge (e)	Energy** (keV)	Time-of-flight (ns)	$\Delta_{m/q}/(m/q)$ (FWHM)	Δ_m/m (FWHM)
H	1	1	26	38.5	0.052	0.472
He	4	2	52	53.1	0.043	0.253
C	12	6	143	52.6	0.035	0.163
N	14	7	164	52.6	0.035	0.167
O	16	6	131	60.2	0.035	0.221
Ne	20	8	166	58.1	0.028	0.220
Si	28	9	174	64.1	0.028	0.246
S	32	10	189	64.9	0.028	0.254
Fe	56	11	157	79.3	0.026	0.302

*For 440 km s^{-1} solar wind speed and 30 kV post-acceleration.
**Measured by solid-state detector.

for SWICS was performed in November–December 1995, June 1996, and June 1997 at the University of Bern Accelerator Facility. SWIMS pre-flight calibration was performed in June–July 1996 and June 1997 at the University of Bern. Both SWICS and SWIMS were additionally calibrated at the Justus-Liebig University in Giessen, Germany in April–June 1996. We measured the energy and MCP bias dependence of efficiencies for various ion species, geometrical factors, and the angular and energy responses of the electrostatic deflection systems for both sensors. SWIMS was also checked for temperature effects on HV-noise in the Thermal Vacuum chamber at Bern. The Bern accelerator facility is well suited for the calibration of solar-wind-type instruments. It is possible to obtain uniform, stable beams of gas-derived ion species (H^+, He^+, He^{++}, Ne^{+4}, Ar^{+4}, Kr^{+5}) in the range of 0.5 to 60 keV e^{-1}. The Giessen facility, using an ECR (Electron Cyclotron Resonance) ion source, was used to deliver heavy solar wind ions (Si, S, Na, Fe) as well as high charge-state ions (O^{+5}) to SWICS and a wide range of metals (Ti, Ni, Co, Zn, Cr) to SWIMS. The SWIMS flight spare unit is available for extensive calibrations with heavy metal ion beams after the launch of ACE.

5.5.1. *SWICS Efficiencies*

Knowledge of the efficiencies of the MCPs as a function of energy of the various elements is required to obtain fluxes and relative abundances of solar wind ions. The stop efficiencies of SWICS for He, C, O, Ar, and Kr as a function of energy from 0.5 to 20 keV amu^{-1} are shown in Figure 15. Start efficiencies have a similar energy and species dependence.

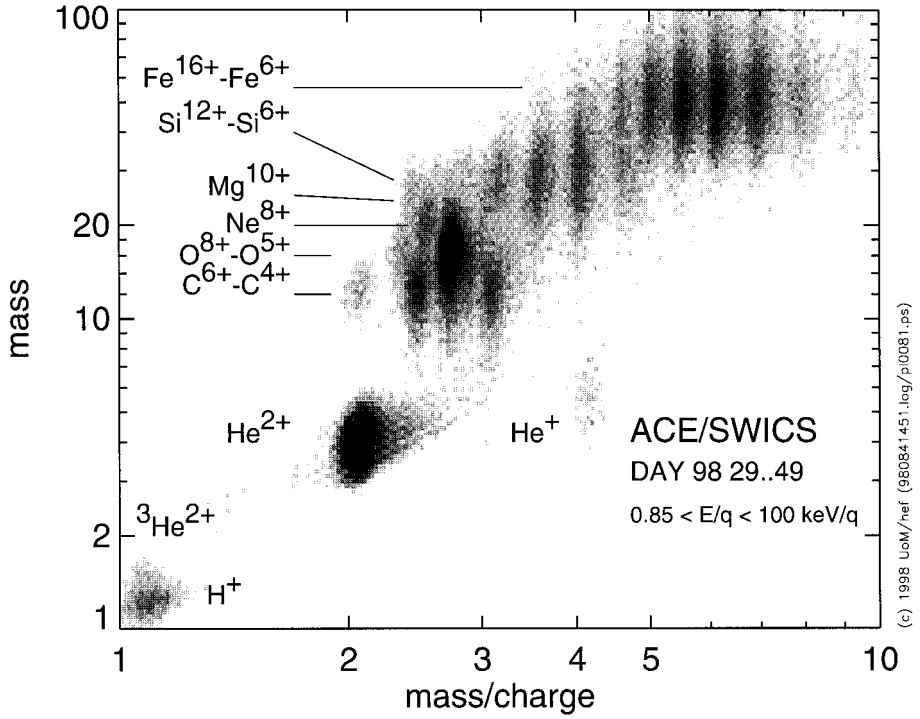

Figure 13. Display of the mass vs mass-per-charge distributions of solar wind ions derived from the raw energy and time-of-flight pulse-height data collected by SWICS during days 29–49 of 1998. The mass and mass/charge values were computed on the ground using algorithms identical to those employed by the S^3DPU for the on-board classification of solar wind ions. The density profiles show well-resolved peaks of the major solar wind heavy elements and their dominant charge states. The relative abundances of the various charge states of elements that can be derived from data such as shown here may be used to infer the temperatures and temperature profiles of the low solar corona.

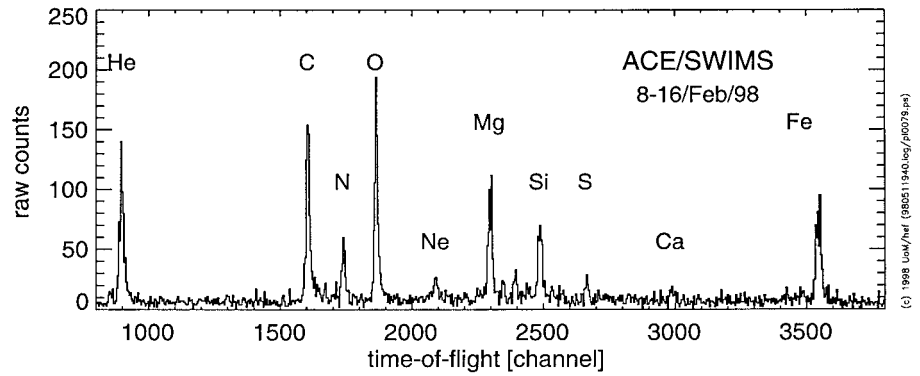

Figure 14. Display of the mass distribution of solar wind ions derived from the raw time-of-flight pulse-height data collected by SWIMS.

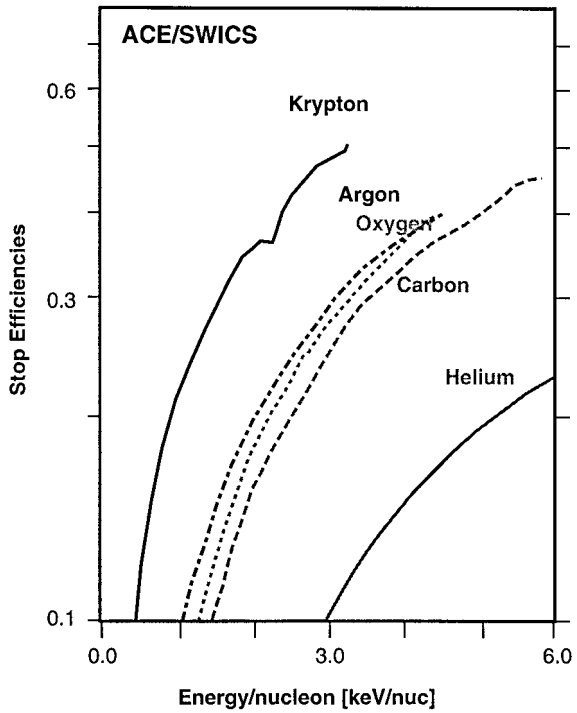

Figure 15. Measured dependence of the SWICS stop efficiency on energy per nucleon for the indicated elements derived from calibration data. The stop efficiency is the ratio of the Double Coincidence Rate to the Start Rate and reflects the effects of ion scattering caused by the carbon foil, the efficiency of generating back-scattered secondary electrons from the solid-state detectors and adjacent surfaces, the efficiency of focusing these electrons onto the stop microchannel plate (MCP), and the efficiency of detecting these electrons by the stop MCP.

5.5.2. *SWIMS Elemental and Isotopic Resolution*

SWIMS has excellent mass resolution, which allows it to resolve all the solar wind elements and isotopes up to and including Ni. Figure 16 shows the mass resolution of SWIMS, which resolves peaks for C (from the thin carbon foil), Ne (the primary gas in the plasma), Mg, Ti, Ni, Zn, and Rb. There are no significant isotope peaks due to the mass-per-charge selection of the bending magnets in the calibration facility. Figure 17 shows raw calibration data measured with the SWIMS spare unit that shows clearly resolved isotopes of Ne. Notice that a fraction of the Ne ions become doubly charged as they pass though the carbon foil.

6. Browse Parameter Data

The SWICS/SWIMS investigation will provide selected solar wind parameters for several heavy ion species averaged over 12 min (or multiples of 12 min). The following data will be included:

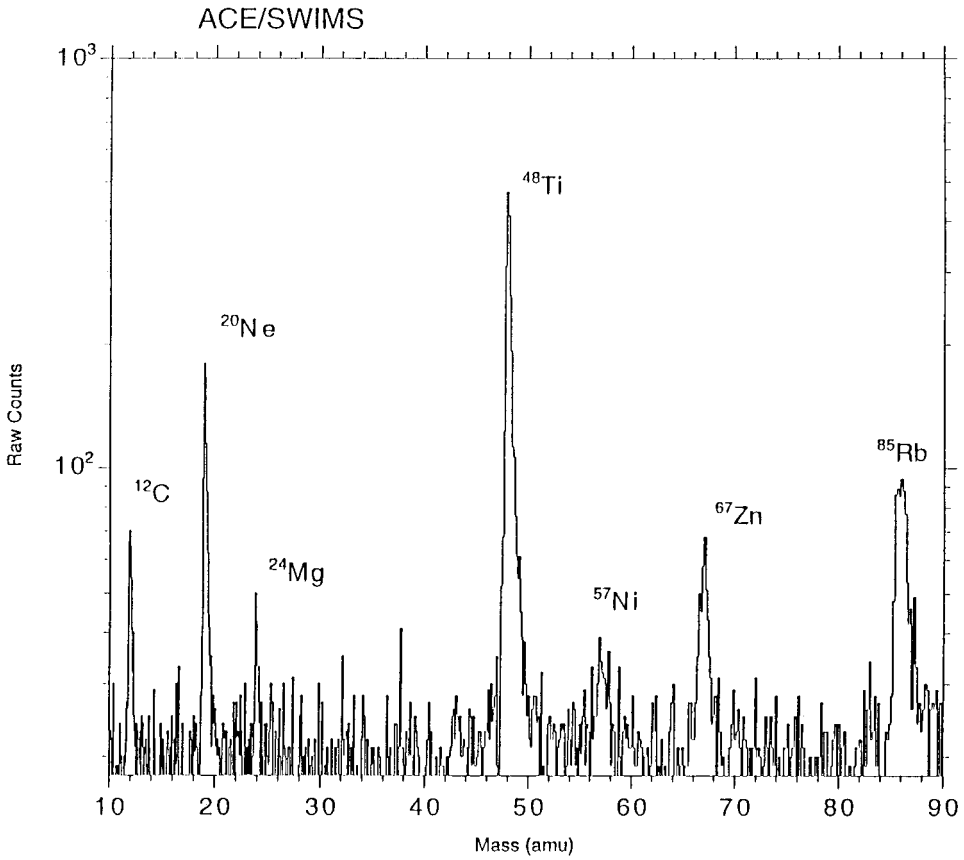

Figure 16. Mass spectrum obtained by SWIMS during calibration using an alloy rod as the primary ion source. Several peaks from the sample (Mg, Ti, Ni, Zn, Rb) are clearly resolved, as well as a Neon peak from the ionizing gas. A Carbon peak is also present from ions knocked out of the thin carbon foil at the entrance of the instrument.

(1) Bulk speed and kinetic temperature of solar wind He^{++} and O^{6+}.
(2) Coronal electron freezing-in temperature derived from O^{6+}/O^{7+}.
(3) Fe/O (Low FIP/ High FIP) abundance ratio.
(4) He/O abundance ratio.

7. Summary

The SWICS/SWIMS Investigation on the ACE spacecraft will obtain detailed information on the thermal and suprathermal ion populations in the solar wind upstream of the Earth's magnetosphere, with an emphasis on compositions of these plasmas. This information is required for studies of a variety of solar, heliospheric and interstellar phenomena, and is important for interpreting results from other

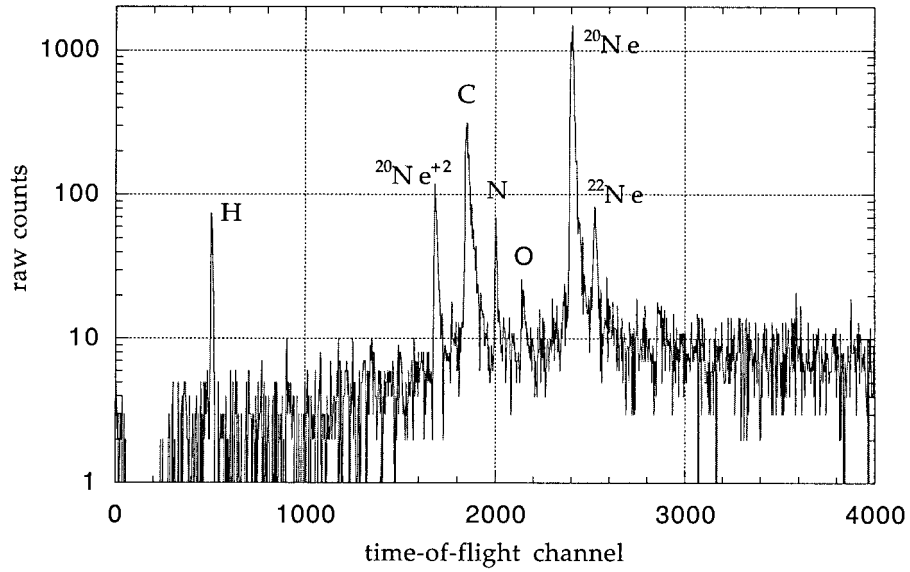

Figure 17. Display of the isotopic resolution of Neon derived from calibration data using Ne^{4+} as a primary beam.

heliospheric missions such as *Ulysses*, ISTP spacecraft such as WIND and SOHO, and various space and ground-based observations of the solar photosphere and lower corona. These data, especially in combination with measurements from other instruments on ACE, other GGS and ISTP spacecraft and *Ulysses*, as well as ground and space observations of the Sun, will make possible a number of new studies of solar, heliospheric and magnetospheric phenomena. These scientific objectives require measurements provided by the two complementary instruments of this investigation. The Solar Wind Ion Composition Spectrometer (SWICS) will determine routinely and with good time resolution the charge states and distribution functions of the most abundant solar wind heavy ions (H, He, C, O, Ne, Mg, Si, and Fe) from 0.5 to 30 keV e^{-1}, and will measure pickup ions of interplanetary and interstellar origin. The Solar Wind Ion Mass Spectrometer (SWIMS) will measure the elemental and isotopic composition and charge state of the solar wind plasma with far greater precision than is possible with SWICS (i.e., elements Na, Al, S, Ar, Ca, Cr, and Ni, and isotopes of Ne, Mg, Si, S, Ar, Ca, and Fe).

Acknowledgements

The development of the SWICS and SWIMS experiments was an international effort involving the Space Physics group in the Department of Physics at the University of Maryland, the Physikalisches Institut of the Universität Bern in Bern,

Switzerland, and the Institut für Datenverarbeitungsanlagen of the Universität Braunschweig in Braunschweig, Germany. Many individuals at these institutions contributed greatly in the design, development, fabrication, testing, and calibration of the two instruments and the S^3DPU. We are particularly grateful to the following individuals: At the University of Maryland to Fred Wire for the design and testing of digital subsystems for both instruments; to Richard Pappalardo for the developing and testing the power systems for SWIMS; to Bob Cates and Charles Tomasevich for the mechanical design of SWICS and SWIMS; to Maurice Pairel and Pota Floros who did an excellent job laying out and assembling the wiring harnesses and the many electronics boards for the instruments; to Scott Lasley for his laboratory testing of sensor detectors and for his invaluable support during the integration, testing and calibrations of the instruments; to Wayne Shanks and Jeff Miller for their help during instrument testing and calibration; to Pat Ipavich and Jo Ann Simms for the financial management and reporting for the experiments. At the University of Bern to Kurt Bratschi and Paul Liechti, who developed, fabricated and tested the deflection systems for SWIMS and SWICS, including the SWICS entrance collimator and deployable cover; to Raoul Pärli, Rosmarie Neukomm, Olivier Kern, and Peter Wurz for their assistance during the calibrations of SWIMS and SWICS both in Bern and in Giessen; and to Urs Schwab, Martin Steinacher, and Adrian Etter for the operation of the Bern Calibration Facility during the many 24-hour days of calibrations of the instruments. At the Technical University of Braunschweig to Wolfgang Wiewesiek for the electrical design and testing of the DPU hardware; to Bjoern Fiethe for the design and testing of the EGSE hardware; and to Kay-Uwe Reiche and Kai Stöckner who wrote and debugged the extensive DPU software. At the Justus-Liebig University in Giessen, Germany to Professor Dr Erhard Salzborn, Roland Trassl, and Frank Broetz for their valuable and generous support during the testing there. We would like to thank Bruce Williams and Julie Krein of the Applied Physics Laboratory (APL) for their thermal design of both instruments. APL's spacecraft team, led by Mary Chiu and Judi von Mehlem, was also of great assistance from the beginning. In particular, we recognize the extraordinary efforts of James Roberts, Joseph Staiger, and Elliot Rodberg and their integration and test teams, without whose support and flexibility, the quality of SWICS and SWIMS experiments would surely have suffered. We appreciate the support of the ACE Project Office at the Goddard Space Flight Center, headed by Mr Don Margolies, and of the ACE management team at the California Institute of Technology, led by Mr Al Frandsen, throughout the long years of development and preparation of the SWICS and SWIMS experiments. The SWICS and SWIMS investigations were funded by NASA through contract NAS5-32626, by

the Swiss National Science Foundation, and by the Bundesminister für Forschung und Technologie in Germany.

References

Breneman, H. H. and Stone, E. C.: 1985, *Astrophys. J.* **299**, L57.
Bürgi, A. and Geiss, J.: 1986, *Solar Phys.* **103**, 347.
Burlaga, L. F.: 1984, *Space Sci. Rev.* **39**, 255.
Collier, M. R., Hamilton, Gloeckler, G., Bochsler, P., and Sheldon, R. B.: 1996, *Geophys. Res. Lett.* **23**, 1191.
Fisk, L. A., Schwadron, N. A., and Gloeckler, G.: 1997, *Geophys. Res. Lett.* **24**, 93.
Fisk, L. A., Schwadron, N. A., and Zurbuchen, T. H.: 1998, *Space Sci. Rev.* **86**, 51.
Galvin, A. B., Ipavich, F. M., Gloeckler, G., Hovestadt, D., Bame, S. J., Klecker, B., Scholer, M., and Tsurutani, B. T.: 1987, *J. Geophys. Res.* **92**, 12069.
Geiss, J. and Bürgi, A.: 1986, *Astron. Astrophys.* **159** 1.
Geiss, J., Bühler, F., Cerutti, H., Eberhardt, P., and Filleux, C.: 1972, *Sec. 14 of the Apollo 16 Preliminary Science Report* **NASA SP-315**.
Geiss, J., Gloeckler, G., von Steiger, R., Balsiger, H., Fisk, L. A., Galvin, A. B., Ipavich, F. M., Livi, S., McKenzie, J. F., Ogilvie, K. W., Wilken, B.: 1995, *Science* **268**, 1033.
Geiss, J., Gloeckler, G., and von Steiger, R.: 1996, in R. von Steiger, R. Lallement, and M. A. Lee (eds), 'The Heliosphere in the Local Interstellar Medium, Proceedings of the First ISSI Workshop', *Space Sci. Rev.* **78**, 43.
Gloeckler, G.: 1977, University of Maryland Technical Report TR 77-043 (unpublished).
Gloeckler, G.: 1990, *Rev. Sci. Instrum.* **61** , 3613.
Gloeckler, G.: 1996, in R. von Steiger, R. Lallement, and M. A. Lee (eds), 'The Heliosphere in the Local Interstellar Medium, Proceedings of the First ISSI Workshop', *Space Sci. Rev.* **78**, 335.
Gloeckler, G. and Geiss, J.: 1989, in J. C. Waddington (ed.), *AIP Conf. Proceedings* **183**, 49.
Gloeckler, G. and Geiss, J.: 1998, *Space Sci. Rev.* **86**, 127.
Gloeckler, G. and Hsieh, K. C.: 1979, *Nucl. Inst. Meth.* **165**, 537.
Gloeckler, G., Geiss, J., Balsiger, H., Fisk, L. A., Gliem, F., Ipavich, F. M., Ogilvie, K. W., Stüdemann, W., and Wilken, B.: 1983, *ESA Spec. Publ.* **SP-1050**, 77.
Gloeckler, G., Ipavich, F. M., Stüdemann, W., Wilken, B., Hamilton, D. C., Kremser, G., Hovestadt, D., Gliem, F., Lundgren, R. A., Rieck, W., Tums, E. D., Cain, J. C., Masung, L. S., Weiss, W., and Winterhof, P.: 1985, *IEEE Trans. on Geosci. and Remote Sensing* **GE-233**, 234.
Gloeckler, G., Hovestadt, D., Ipavich, F. M., Scholar, M., Clicker, B., and Galvin, A. B.: 1986, *Geophys. Res. Letters* **13**, 251.
Gloeckler, G., Ipavich, F. M., Hamilton, D. C., Wilken, B., and Kremser, G.: 1989, *EOS Trans.* **70**, 424.
Gloeckler, G., Geiss, J., Balsiger, H., Bedini, P., Cain, J. C., Fischer, J., Fisk, L. A., Galvin, A. B., Gliem, F., Hamilton, D. C., Hollweg, J. V., Ipavich, F. M., Joos, R., Livi, S., Lundgren, R. A., Mall, U., McKenzie, J. F., Ogilvie, K. W., Ottens, F., Rieck, W., Tums, E. O., von Steiger, R., Weiss, W., and Wilken, B.: 1992, *Astron. Astrophys. Suppl. Ser.* **92**, 267.
Gloeckler, G., Geiss, J., Balsiger, H., Fisk, L. A., Galvin, A. B., Ipavich, F. M., Ogilvie, K. W., von Steiger, R., and Wilken, B.: 1993, *Science* **261**, 70.
Gloeckler, G., Schwadron, N. A., Fisk, L. A., and Geiss, J.: 1995a, *Geophys. Res. Lett.* **22**, 2665.
Gloeckler, G., Balsiger, H., Bürgi, A., Bochsler, P., Fisk, L. A., Galvin, A. B., Geiss, J., Gliem, F., Hamilton, D. C., Holzer, T. E., Hovestadt, D., Ipavich, F. M., Kirsch, E., Lundgren, R. A., Ogilvie, K. W., Sheldon, R. B., and Wilken, B.: 1995b, *Space Sci. Rev.* **71**, 79.

Habbal, S. R., Esser, R., Guhathakurta, M., and Fisher, R. P.: 1995, *Geophys. Res. Lett.* **22**, 1465.
Hamilton, D. C., Gloeckler, G., Ipavich, F. M., Lundgren, R. A., Sheldon, R. B., and Hovestadt, D.: 1990, *Rev. Sci. Instrum.* **61**, 3104.
Hilchenbach, M., Hovestadt, D., Klecker, B., Möbius, E.: 1991, *Proceedings Solar Wind Seven (E. Marsch, G. Schwenn ,ed.), Goslar, Germany, Pergamon Press* **349**.
Hollweg, J. V.: 1978, *Rev. Geophys. Space Phys.* **16**, 689.
Hovestadt, D., Hilchenbach, M., Bürgi, A., Klecker, B., Laeverenz, P., Scholer, M., Grünwaldt, H., Axford, W. I., Livi, S., Marsch, E., Wilken, B., Winterhoff, H. P., Ipavich, F. M., Bedini, P., Coplan, M. A., Galvin, A. B., Gloeckler, G., Bochsler, P., Balsiger, H., Fischer, J., Geiss, J., Kallenbach, R., Wurz, P., Reiche, K. U., Gliem, F., Judge, D. L., Ogawa, H. S., Hsieh, K. C., Möbius, E., Lee, M. A., Managadze, G. G., Verigin, M. I., and Neugebauer, M.: 1995, *Solar Phys.* **162**, 441.
Hundhausen, A., Gilbert, H., and Bame, S.: 1968, *J. Geophys. Res.* **73**, 5485.
Ipavich, F. M., Lundgren, R. A., Lambird, B. A., and Gloeckler, G.: 1978, *Nucl. Inst. and Meth.* **154**, 291.
Ipavich, F. M., Galvin, A. B., Gloeckler, G., Scholer, M., and Hovestadt, D.: 1981, *J. Geophys. Res.* **86**, 4337.
Ipavich, F. M, Galvin, A. B., Gloeckler, G., Hovestadt, D., Klecker, B., and Scholer, M.: 1986, *Science* **232**, 366.
Isenberg, P. A., and Hollweg, J. V.: 1983, *J. Geophys. Res.* **88**, 3923.
Isenberg, P. A.: 1991, *J. Geophys. Res.* **96**, 155.
Marsden, R. G., Sanderson, T. R., Tranquille, C., Wenzel, K.-P., and Smith, E. J.: 1987, *J. Geophys. Res.* **92**, 11009.
Möbius, E., Hovestadt, D., Klecker, B., Scholer, M., Gloeckler, G., and Ipavich, F. M.: 1985, *Nature* **318**, 426.
Möbius, E., Hovestadt, D., Klecker, B., Kistler, L. M., Popecki, M. A., Crocker, K. N., Gliem, F., Granoff, M., Turco, S., Anderson, A., Arbinger, H., Battell, S., Cravens, J., Demain, P., Distelbrink, J., Dors, I., Dunphy, P., Ellis, S., Gaidos, J., Googins, J., Harasim, A., Hayes, R., Humphrey, G., Kastle, H., Kunneth, E., Lavasseur, J., Lund, E. J., Miller, R., Murphy, G., Pfeffermann, K., Reiche, K.-U., Sartori, E., Schimpfle, J., Seidenschwang, E., Shappirio, M., Stockner, K., Taylor, S. C., Vachon, P., Vosbury, M., Wiewesiek, and Ye, V. 1998, 'The Solar Energetic Particle Ionic Charge Analyzer (SEPICA) and the Data Processing Unit (S3DPU) for SWICS, SWIMS and SEPICA', *Space Sci. Rev.* **86**, 449.
Möbius, E., Rucinski, D., Hovestadt, D., and Klecker, B.: 1995, *Astron. Astrophys.* **304**, 505.
Möbius, E., Rucinski, D., Lee, M. A., and Isenberg, P. A.: 1997, *J. Geophys. Res.* (submitted).
Neugebauer, M.: 1981, *Fundamentals of Cosmic Physics* **7**, 131.
Ogilvie, K. W., Bochsler, P., Geiss, J, and Coplan, M. A.: 1980, *J. Geophys. Res.* **85**, 6069.
Reames, D. V., Richardson, I. G., and Barbier, L. M.: 1991, *Astrophys. J.* **382**, L43.
Schmidt, W. K. H., Rosenbauer, H., Shelley, E. G., and Geiss, J.: 1980, *Geophys. Res. Lett.* **7**, 697.
Tan, L. C., Mason, G. M., Klecker, B., and Hovestadt, D.: 1989, *Astrophys. J.* **345**, 572.
von Steiger, R., and Geiss, J.: 1989, *Astron. Astrophys.* **225**, 222.
von Steiger, R., Christon, S. P., Gloeckler, G., and Ipavich, F. M.: 1992, *Astrophys. J.* **389**, 791.
Vauclair, S., and Meyer, J.-P.: 1985, *Proc. 19th Int. Cosmic Ray Conf.* **4**, 233.